Lecture 3
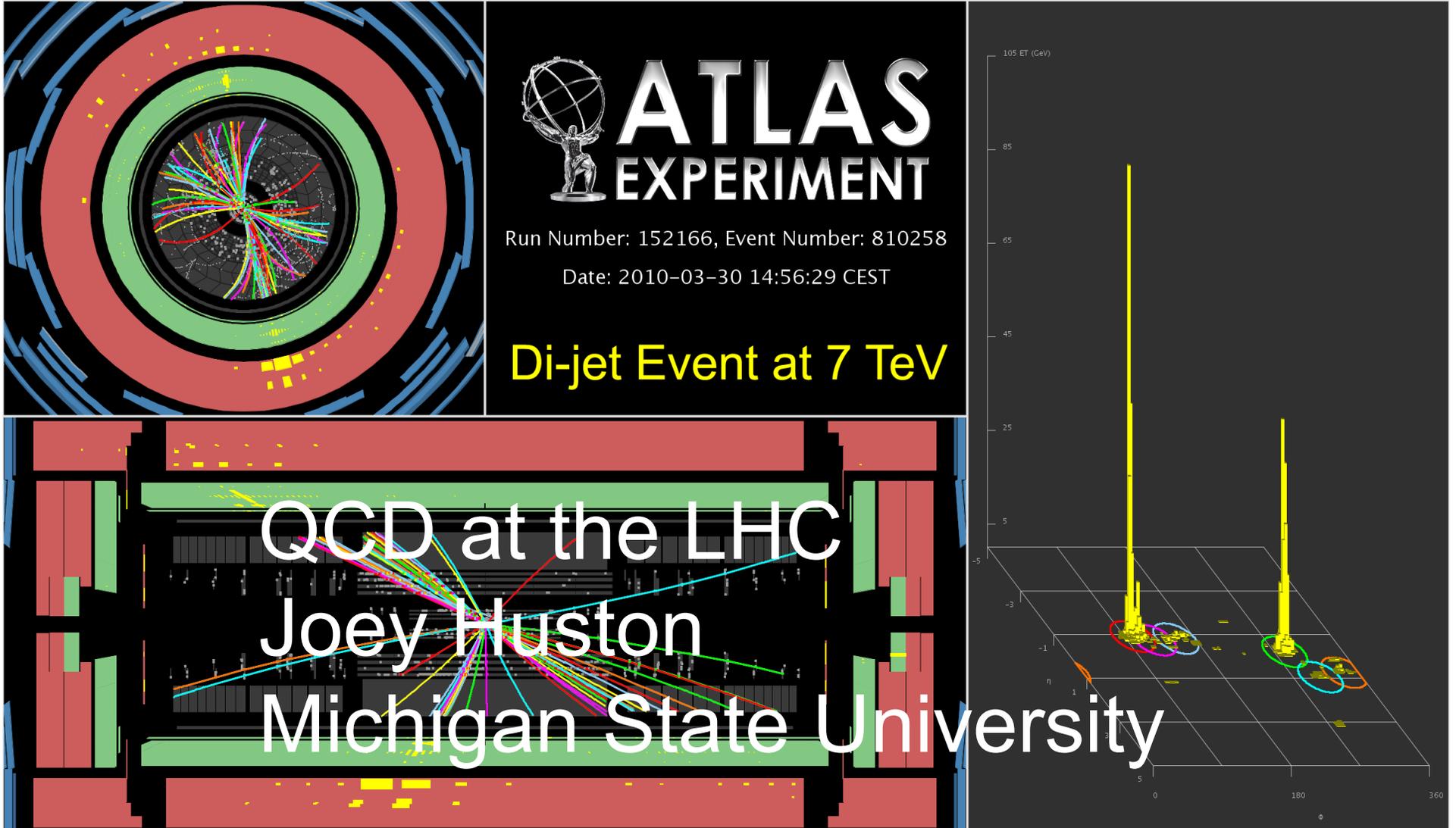

QCD at the LHC
Joey Huston
Michigan State University

Why stop at NLO?

- NNLO is even better, but also more complicated
- Expect (even further) reduced scale dependence
- And in some cases, extra cross section contributions, such as for Higgs production
- Have only been carried out for a few processes to date
- Would really like to have it for inclusive jet production, for example
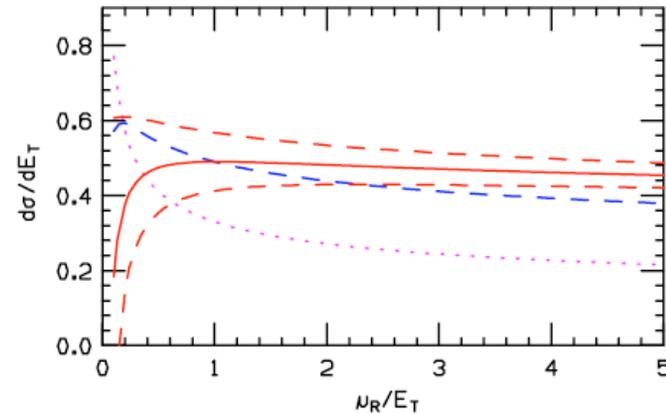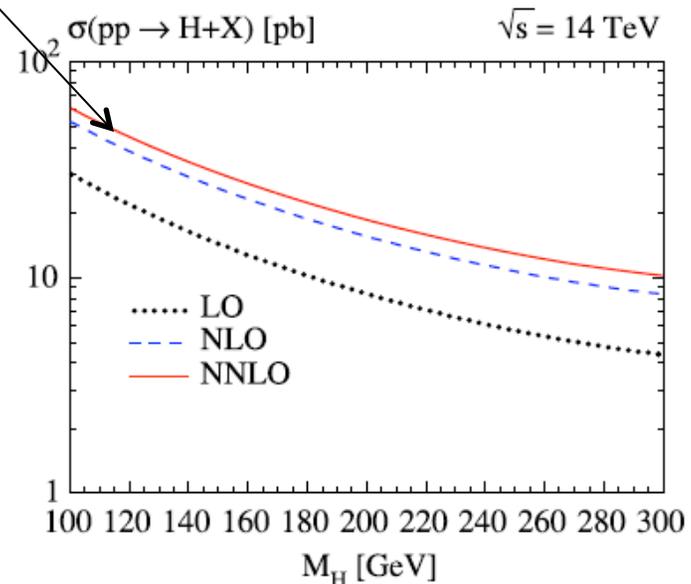 - currently > 8 year project

Figure 16. The single jet inclusive distribution at $E_T = 100\,\text{GeV}$, appropriate for Run I of the Tevatron. Theoretical predictions are shown at LO (dotted magenta), NLO (dashed blue) and NNLO (red). Since the full NNLO calculation is not complete, three plausible possibilities are shown.

$\sigma(pp \rightarrow H+X)$ [pb] $\sqrt{s} = 14\,\text{TeV}$
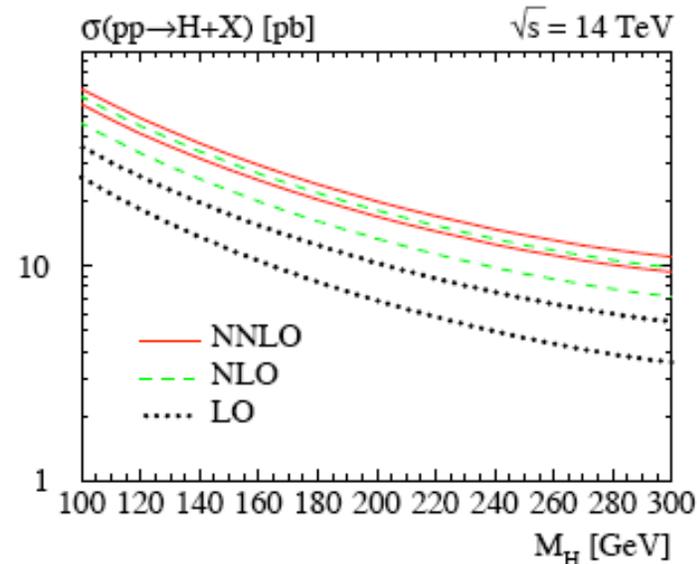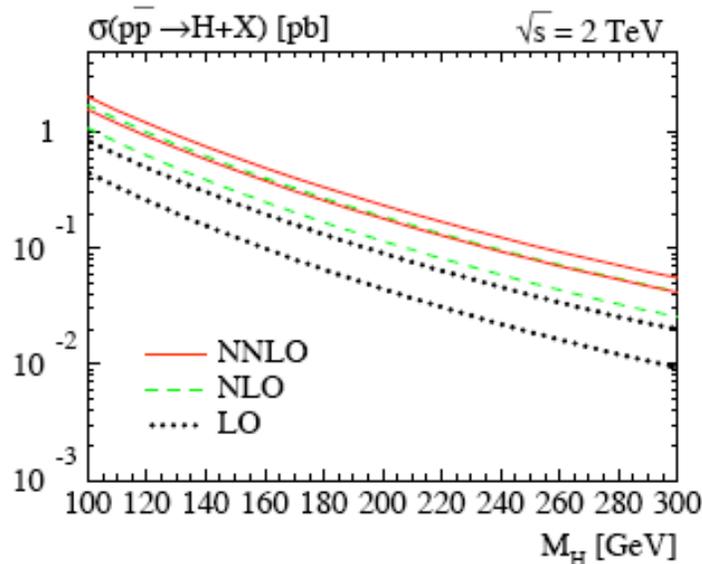
LO
NLO
NNLO

M_H [GeV]

Higgs: LO->NLO->NNLO

(R. Harlander, W. Kilgore, PRL 88 (2002) 201801)
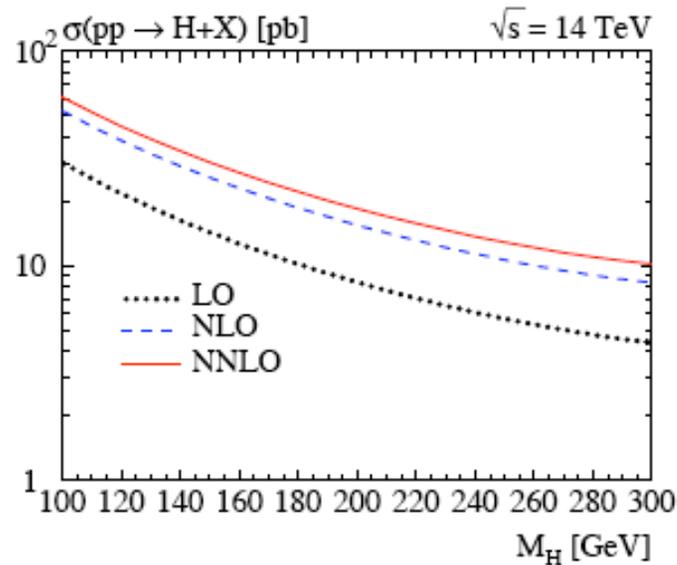
convergence in going:

$$LO \longrightarrow NLO \longrightarrow NNLO$$

Confirmed by the full scale dependence:

$$\Downarrow$$

Note that the NLO result is not covered by the LO error band

All-orders approaches

- Rather than systematically calculating to higher and higher orders in the perturbative expansion, can also use a number of all-orders approaches

- In resummation, dominant contributions from each order in perturbation theory are singled out and resummed by use of an evolution equation

- Near boundaries of phase space, fixed order calculations break down due to large logarithmic corrections, and these contributions can become important. Resummation takes them into account.

- Consider W production
  - one large logarithm associated with production of vector boson close to threshold
  - takes form of $\alpha_s^n \log^{2n-1}(1-z)/(1-z)$ where $z=Q^2/s-1$
  - other large logarithm is associated with recoil of vector boson at very small p_T
  - logarithms appear as $\alpha_s^n \log^{2n-1}(Q^2/p_T^2)$

In both cases there is a restriction of phase space for gluon emission and thus the logs become large and are crucial for an accurate prediction
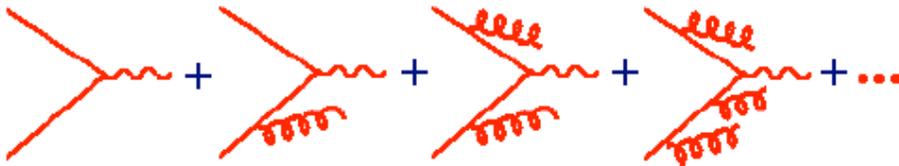
All-orders approaches

- Remember the expression we had after adding gluons on to the W + 1 jet process
  - each gluon added yields an additional factor of α_s and two new logarithms

$$\mathrm{d}\sigma = \sigma_0(W + 1\ \mathrm{jet})\left[1 + \alpha_S(c_{12}L^2 + c_{11}L + c_{10})\right.$$
$$\left. + \alpha_S^2(c_{24}L^4 + c_{23}L^3 + c_{22}L^2 + c_{21}L + c_{20}) + \cdots\right]$$

  - q_T resummation is resumming the effects of logs of Q^2/p_T^2

  - note that q_T resummation does not change the size of the cross section; it just modifies the p_T distribution of the W

- These are the leading logs (LL) (highest power of log for each power of α_s)
- These are the next-to-leading logs (NLL) (next highest power of log…)
  - …and so on
- We know the structure of the LL's, NLL's, NNLL's
- But we don't know the c_{ij} factors until we do the finite order calculation
- LO gives us the LL
- NLO gives us the NLL
  - …and so on
- The accuracy of the resummation improves with the addition for further higher order information
- A resummation program like ResBos has NNLL accuracy

All-orders approaches

- Remember the expression we had after adding gluons on to the W + 1 jet process

  - each gluon added yields an additional factor of α_s and two new logarithms

$$d\sigma = \sigma_0(W + 1 \text{ jet})\left[1 + \alpha_S(c_{12}L^2 + c_{11}L + c_{10})\right.$$
$$\left. +\alpha_S^2(c_{24}L^4 + c_{23}L^3 + c_{22}L^2 + c_{21}L + c_{20}) + \cdots\right]$$

- q_T resummation is resumming the effects of logs of Q^2/p_T^2

- note that q_T resummation does not change the size of the cross section; it just modifies the p_T distribution of the W

- Expression for W boson transverse momentum in which leading logarithms have been resummed to all orders is given by

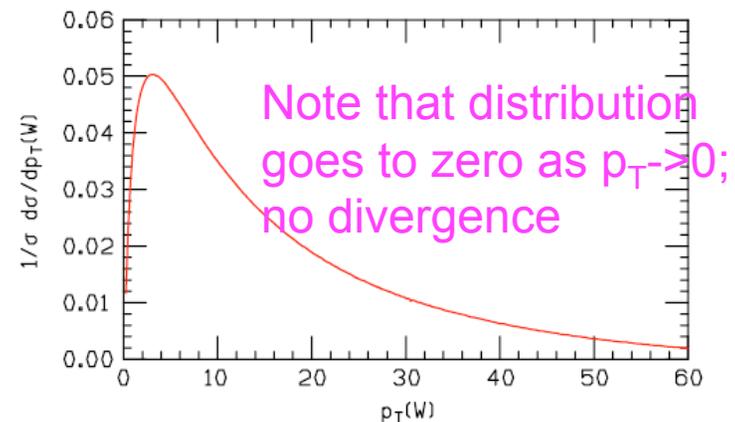$$\frac{d\sigma}{dp_T^2} = \sigma \frac{d}{dp_T^2} \exp\left(-\frac{\alpha_S C_F}{2\pi}\log^2 M_W^2/p_T^2\right)$$

Note that distribution goes to zero as p_T->0; no divergence

Figure 20. The resummed (leading log) W boson transverse momentum distribution.

You could get the same predictions by using PDFs in which the transverse momentum (k_T) has not been integrated out

Parton showers

- A different, but related approach for re-summing logarithms, is provided by parton showering
- By the use of the parton showering process, a few partons produced in a hard interaction at a high-energy scale can be related to partons at an energy scale close to Λ_{QCD}.
- At this lower energy scale, a universal non-perturbative model can then be used to provide the transition to hadrons
- Parton showering allows for evolution, using DGLAP formalism, of parton fragmentation function

Parton Cascade

…plus similar for initial state
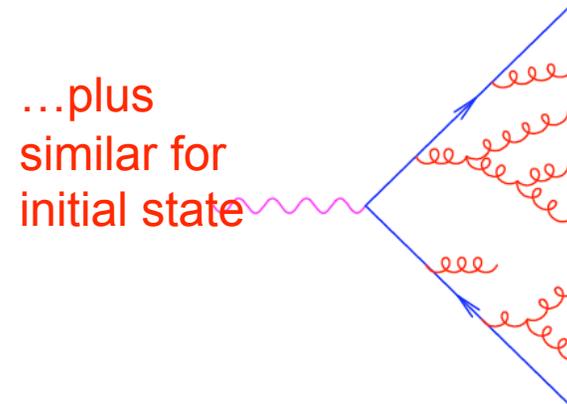
■ Due to successive branching, parton cascade or shower develops. Each outgoing line is source of new cascade, until all outgoing lines have stopped branching. At this stage, which depends on cutoff scale t_0, outgoing partons have to be converted into hadrons via a hadronization model.

- Successive values of an evolution variable t, a momentum fraction z and an azimuthal angle ϕ are generated, along with the flavors of the partons emitted during the parton shower

Parton shower evolution

- On average, emitted gluons have decreasing angles with respect to parent parton directions

  - angular ordering, an aspect of color coherence

- The evolution variable t can be the virtuality of the parent parton [old Pythia and old Sherpa], $E^2(1-\cos\theta)$ where E is the energy of the parent parton and and θ is the opening angle between the two partons [Herwig], or the square of the transverse momentum between the two partons [new Pythia]

$$\theta_1 > \theta_2 > \theta_3$$
$$\theta_1 > \theta_4$$
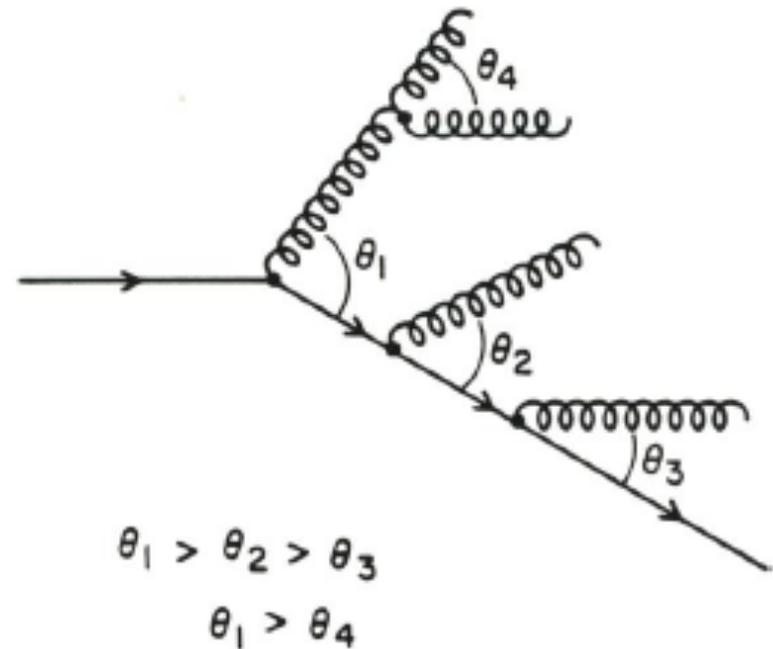
Sudakov form factors

- Sudakov form factors form the basis for both resummation and parton showering
- We can write an expression for the Sudakov form factor of an initial state parton in the form below, where t is the hard scale, t_0 is the cutoff scale and $P(z)$ is the splitting function

$$\Delta(t) \equiv \exp\left[-\int_{t_0}^{t} \frac{dt'}{t'} \int \frac{dz}{z} \frac{\alpha_S}{2\pi} P(z) \frac{f(x/z, t)}{f(x, t)}\right]$$

- Similar form for the final state but without the pdf weighting
- Sudakov form factor resums all effects of soft and collinear gluon emission (so again the double logs), but does not include non-singular regions that are due to large energy, wide angle gluon emission
- Gives the probability **not** to radiate a gluon greater than some energy
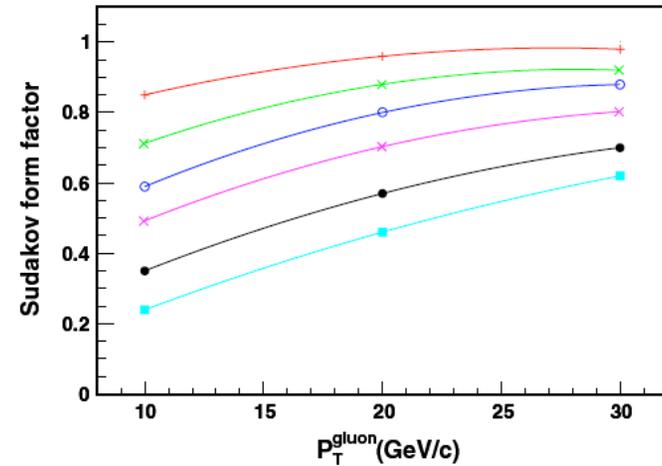- We can draw explicit (approximate) curves for the Sudakov form factors

Figure 21. The Sudakov form factors for initial-state gluons at a hard scale of 100 GeV as a function of the transverse momentum of the emitted gluon. The form factors are for (top to bottom) parton x values of 0.3, 0.1, 0.03, 0.01, 0.001 and 0.0001.

Figure 22. The Sudakov form factors for initial-state gluons at a hard scale of 500 GeV as a function of the transverse momentum of the emitted gluon. The form factors are for (top to bottom) parton x values of 0.3, 0.1, 0.03, 0.01, 0.001 and 0.0001.
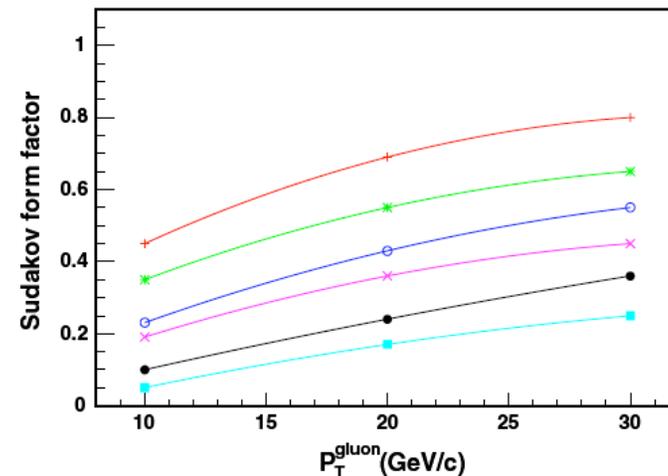
Sudakov form factors

- The Sudakov form factor decreases (the probability of radiating increases) as the p_T of the radiated gluon decreases, as the hardness of the interaction increases, or as the x value of the incoming parton decreases (more phase space for gluon radiation)
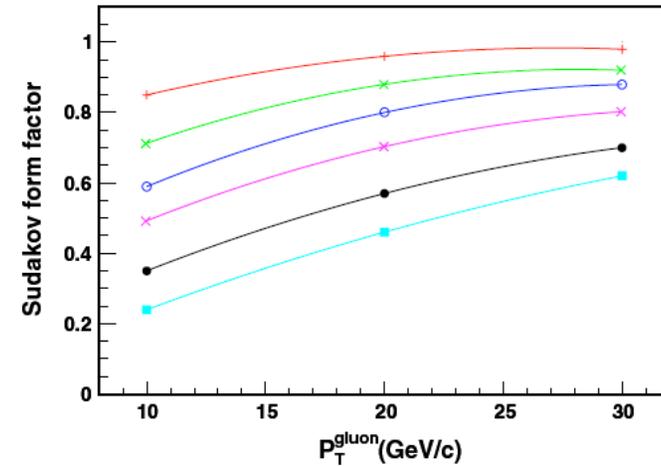

Figure 21. The Sudakov form factors for initial-state gluons at a hard scale of 100 GeV as a function of the transverse momentum of the emitted gluon. The form factors are for (top to bottom) parton x values of 0.3, 0.1, 0.03, 0.01, 0.001 and 0.0001.

Figure 22. The Sudakov form factors for initial-state gluons at a hard scale of 500 GeV as a function of the transverse momentum of the emitted gluon. The form factors are for (top to bottom) parton x values of 0.3, 0.1, 0.03, 0.01, 0.001 and 0.0001.

Sudakov form factors: quarks and gluons

so quarks don't radiate as much; it's the C_F compared to C_A

Figure 23. The Sudakov form factors for initial-state quarks at a hard scale of 100 GeV as a function of the transverse momentum of the emitted gluon. The form factors are for (top to bottom) parton x values of 0.3, 0.1 and 0.03.

Figure 21. The Sudakov form factors for initial-state gluons at a hard scale of 100 GeV as a function of the transverse momentum of the emitted gluon. The form factors are for (top to bottom) parton x values of 0.3, 0.1, 0.03, 0.01, 0.001 and 0.0001.
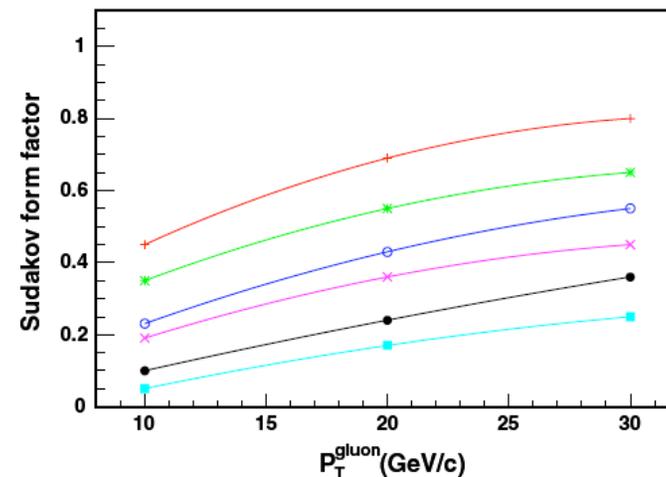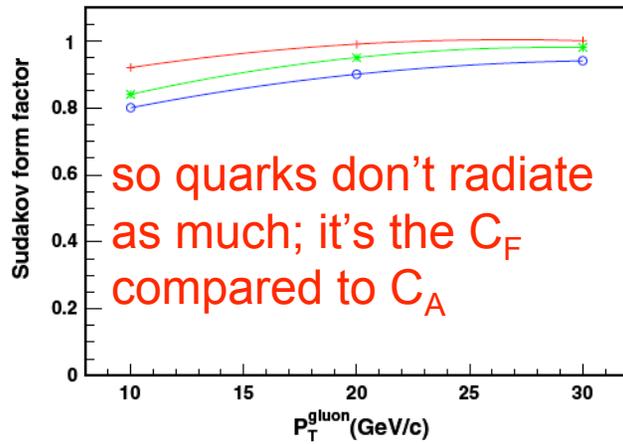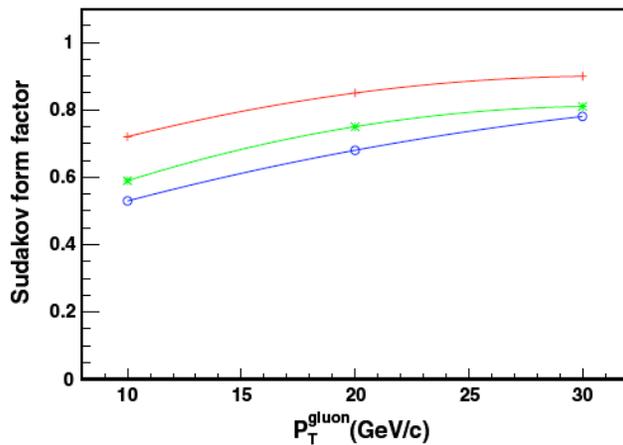

Figure 24. The Sudakov form factors for initial-state quarks at a hard scale of 500 GeV as a function of the transverse momentum of the emitted gluon. The form factors are for (top to bottom) parton x values of 0.3, 0.1 and 0.03.
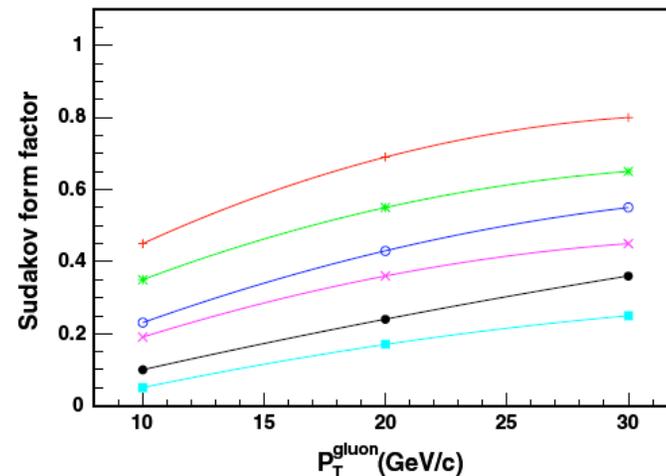
Figure 22. The Sudakov form factors for initial-state gluons at a hard scale of 500 GeV as a function of the transverse momentum of the emitted gluon. The form factors are for (top to bottom) parton x values of 0.3, 0.1, 0.03, 0.01, 0.001 and 0.0001.

Let's take a specific example

- Consider gg fusion production of a 120 GeV Higgs (so use Q=100 GeV) at 7 TeV

- The x values of each of the incoming gluons are in the range from 0.01 to 0.03

- For an ISR jet (gluon) with a p_T of 20 GeV/c or greater, the Sudakov form factor is on the order of 0.7, i.e. there is a 30% chance of radiating such a gluon

- Since there are two incoming gluons, chance of having a jet > 20 GeV/c is ~0.5
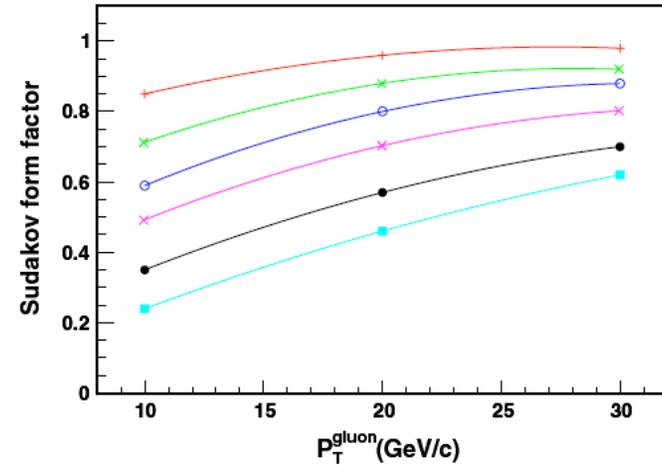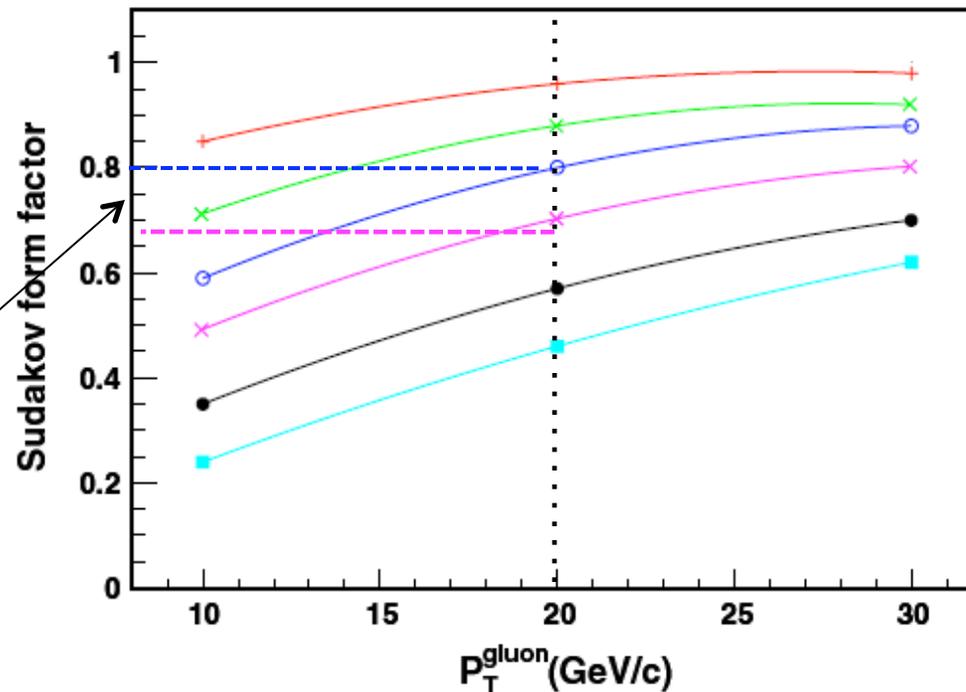

Figure 21. The Sudakov form factors for initial-state gluons at a hard scale of 100 GeV as a function of the transverse momentum of the emitted gluon. The form factors are for (top to bottom) parton x values of 0.3, 0.1, 0.03, 0.01, 0.001 and 0.0001.

Note

- We can only observe emissions above a certain resolution scale
- Below this resolution scale, singularities cancel, leaving a finite remnant
- (some of) the virtual corrections encountered in a full NLO calculation are included by the use of Sudakov suppression between vertices
- So a parton shower Monte Carlo is not purely a fixed order calculation, but has a higher order component as well
- This is a statement that you'll often hear

finite Sudakov emission

virtual   +   real collinear
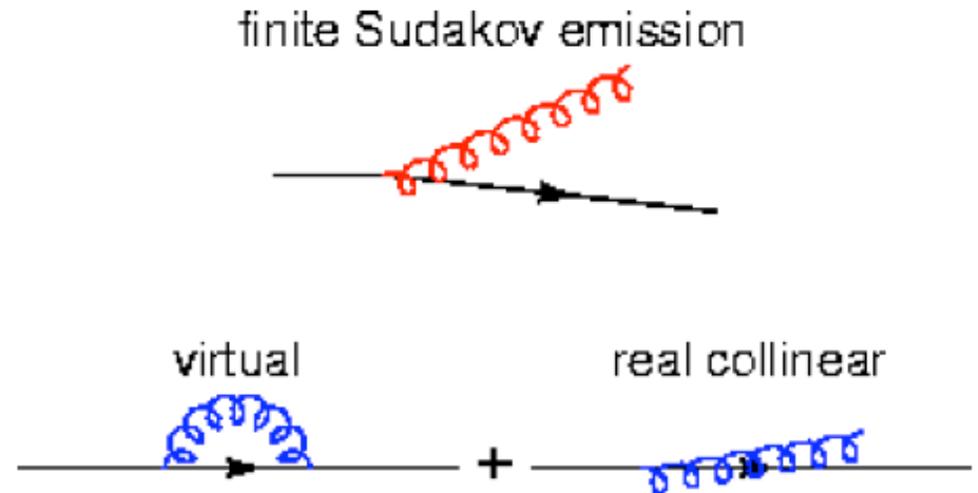
Merging ME and PS approaches

- Parton showers provide an excellent description in regions which are dominated by soft and collinear gluon emission
- Matrix element calculations provide a good description of processes where the partons are energetic and widely separated and also take into account interference effects between amplitudes
  - but do not take into account interference effects in soft and collinear emissions which cannot be resolved, and thus lead to Sudakov suppression of such emissions
- Hey, I know, let's put them together, but we have to be careful not to double-count
  - parton shower producing same event configuration already described by matrix element
  - Les Houches Accord (which I named) allows the ME program to talk to the PS program

Figure 26. In the NLO formalism, the same scale, proportional to the hardness of the process, is used for each QCD vertex. For the case of the $W+2$ jet diagram shown above to the left, a scale related to the mass of the W boson, or to the average transverse momentum of the produced jets, is typically used. The figure to the right shows the results of a simulation using the CKKW formalism. Branchings occur at the vertices with resolution parameters d_i, where $d_1 > d_2 \gg d_{\text{ini}} > d_3 > d_4 > d_5 > d_6$. Branchings at the vertices 1–2 are produced with matrix element information while the branchings at vertices 3–6 are produced by the parton shower.

Merging ME and PS approaches

- A number of techniques to combine, with most popular/correct being CKKW
  - matrix element description used to describe parton branchings at large angle and/or energy
  - parton shower description is used for smaller angle, lower energy emissions
- Division into two regions of phase space provided by a resolution parameter d_{ini}
- Argument of α_s at all of the vertices is taken to be equal to the resolution parameter d_i (showering variable) at which the branching has taken place
- Sudakov form factors are inserted on all of the quark and gluon lines to represent the lack of any emissions with a scale larger than d_{ini} between vertices
  - parton showering is used to produce additional emissions at scales less than d_i
- For typical matching scale, ~10% of the n-jet cross section is produced by parton showering from n-1 parton ME
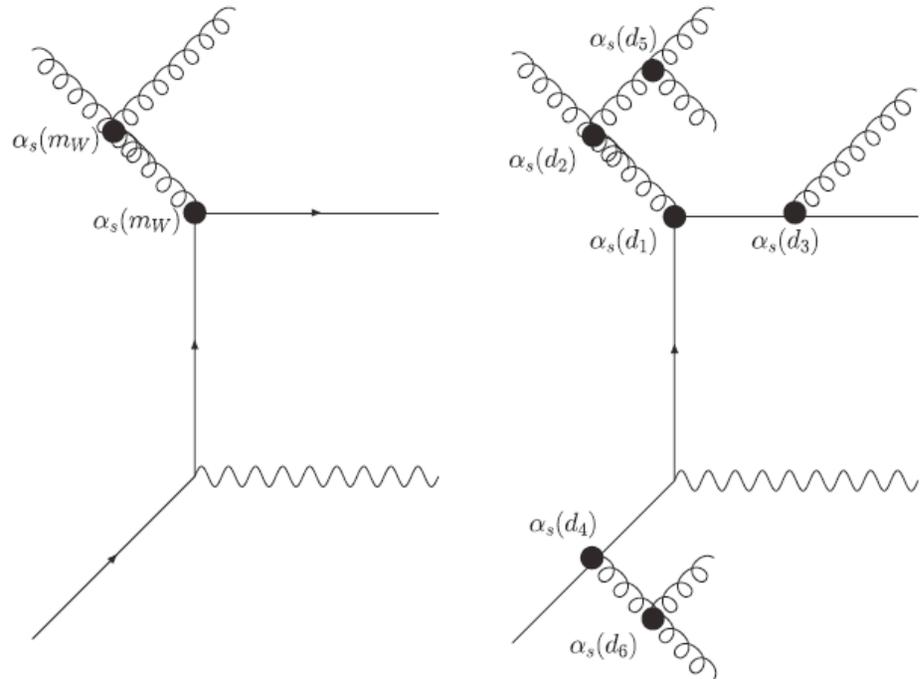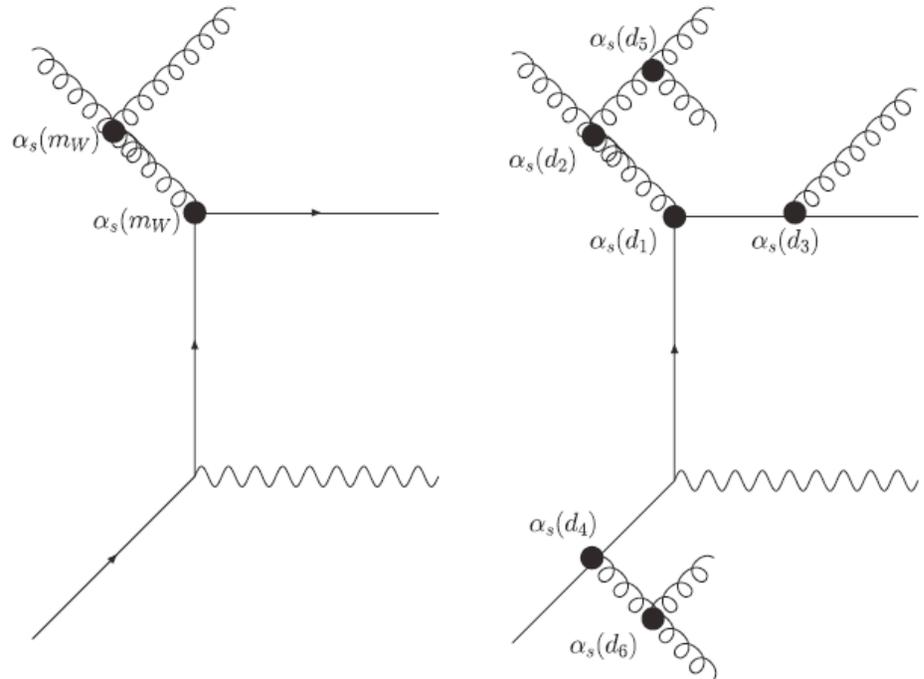

Figure 26. In the NLO formalism, the same scale, proportional to the hardness of the process, is used for each QCD vertex. For the case of the $W+2$ jet diagram shown above to the left, a scale related to the mass of the W boson, or to the average transverse momentum of the produced jets, is typically used. The figure to the right shows the results of a simulation using the CKKW formalism. Branchings occur at the vertices with resolution parameters d_i, where $d_1 > d_2 \gg d_{ini} > d_3 > d_4 > d_5 > d_6$. Branchings at the vertices 1–2 are produced with matrix element information while the branchings at vertices 3–6 are produced by the parton shower.

see Alpgen, Madgraph, Sherpa,…
MLM approach (which I also named) is an approximation to the full CKKW procedure

Best of all worlds: from CHS

NLO + parton shower MC

trick is to find out what parton shower does at NLO, so as not to double-count

with MC@NLO, a small fraction (~10%) of the events have a negative weight (-1)

Several groups have worked on the subject to consistently combine partonic NLO calculations with parton showers.

- Collins, Zu [95, 96].
- Frixione, Nason, Webber (MC@NLO) [97–99].
- Kurihara, Fujimoto, Ishikawa, Kato, Kawabata, Munehisa, Tanaka [100].
- Krämer, Soper [101–103].
- Nagy, Soper [104, 105].

MC@NLO is the only publicly available program that combines NLO calculations with parton showering and hadronization. The HERWIG Monte Carlo is used for the latter. The use of a different Monte Carlo, such as PYTHIA, would require a different subtraction scheme for the NLO matrix elements. The processes included to date are $(W, Z, \gamma^*, H, b\bar{b}, t\bar{t}, HW, HZ, WW, WZ, ZZ)$. Recently, single top hadroproduction has been added to MC@NLO [106]. This is the first implementation of a process that has both initial- and final-state singularities. This allows a more general category of additional processes to be added in the future. Work is proceeding on the addition of inclusive jet production and the production of a Higgs boson via WW fusion. Adding spin correlations to a process increases the level of difficulty but is important for processes such as single top production.

If, in addition, the CKKW formalism could be used for the description of hard parton emissions, the utility and accuracy of a NLO Monte Carlo could be greatly increased. The merger of these two techniques should be possible in Monte Carlos available by the time of the LHC turn-on.

Powheg is a program/technique that results in no negative weight events (or a few); many new processes have been added

But it's still very time(theorist)-consuming to add a new process, and most of the processes so far are 2->1, 2->2

t-tbar in MC@NLO

- At low p_T for the t-tbar system, the cross section is described (correctly) by the parton shower, which resums the large logs near $p_T \sim 0$
- At high p_T, the cross section is described (correctly) by the NLO matrix element
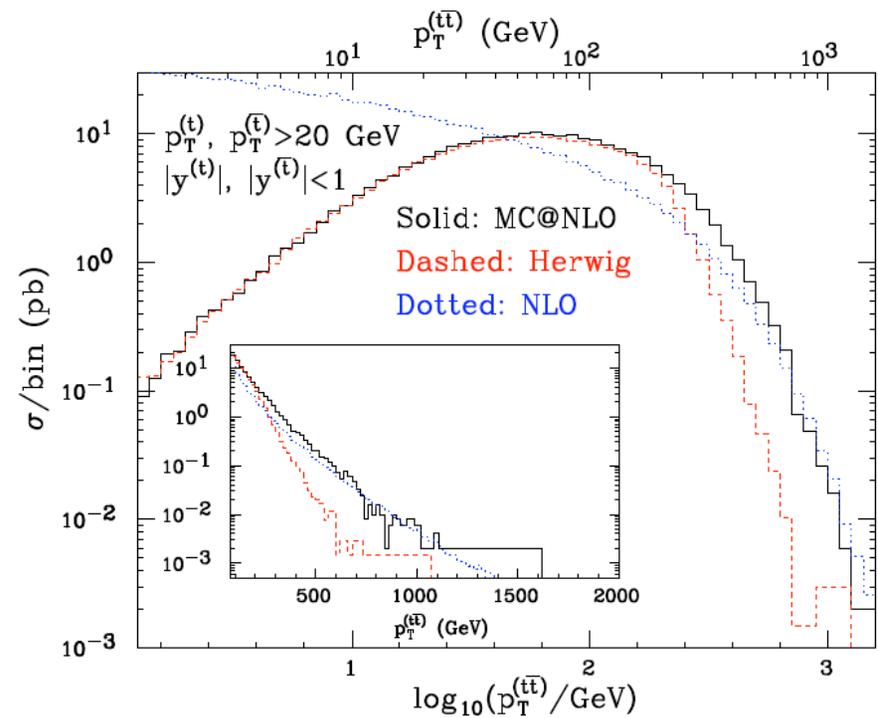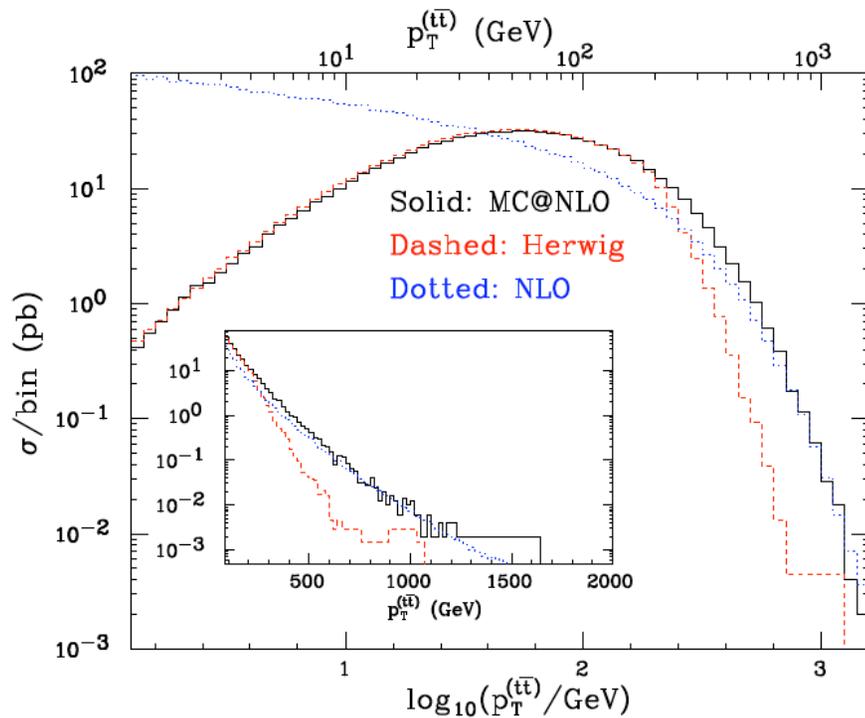
Hadrons and PDFs

- The proton is a dynamical object; the structure observed depends on the time-scale (Q^2) of the observation
- But we know how to calculate this variation (DGLAP)
- We just have to determine the starting points from fits to data
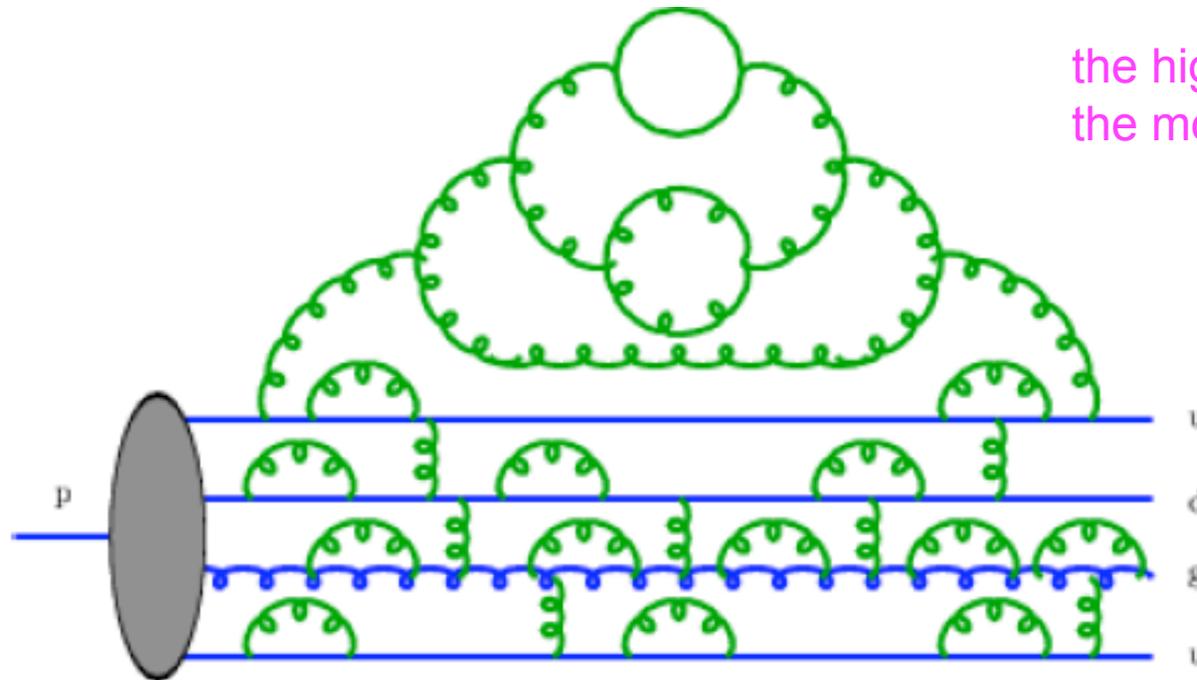
the higher the value of Q^2, the more detail we examine

$$f_i(x, Q^2) = \text{number density of partons } i$$
$$\text{at momentum fraction } x \text{ and probing scale } Q^2$$

Parton distribution functions and global fits

- Calculation of production cross sections at the LHC relies upon knowledge of pdf's in the relevant kinematic region
- Pdf's are determined by global analyses of data from DIS, DY and jet production
- Three major groups that provide semi-regular updates to parton distributions when new data/theory becomes available
  - MRS->MRST98->MRST99 ->MRST2001->MRST2002 ->MRST2003->MRST2004 ->MSTW2008
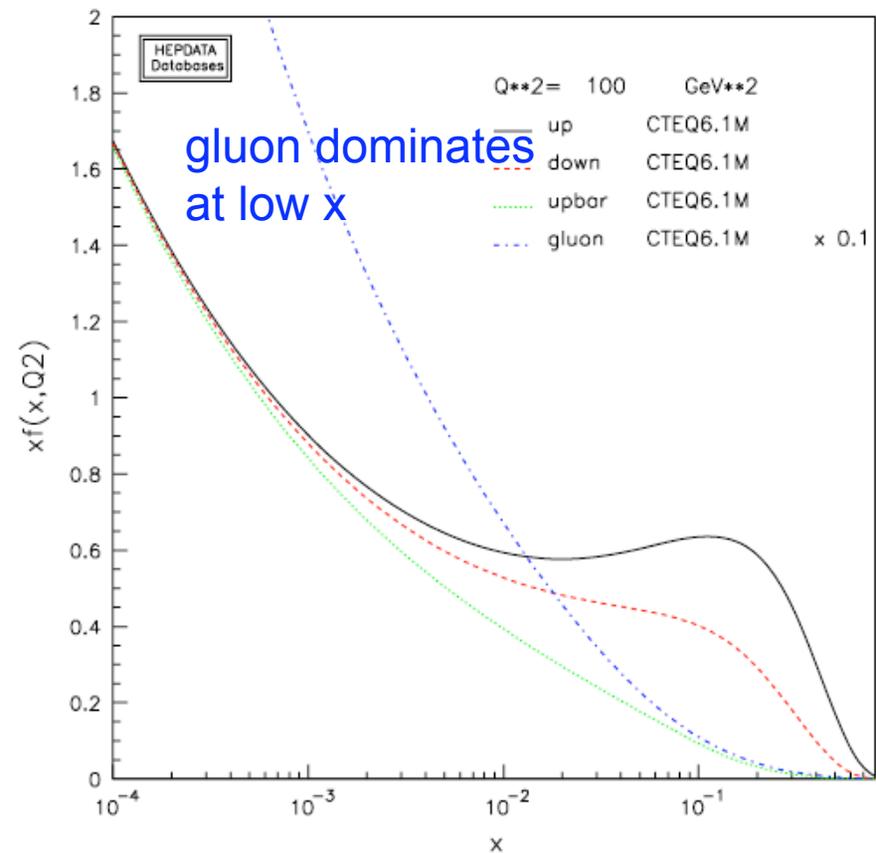 - CTEQ->CTEQ5->CTEQ6 ->CTEQ6.1->CTEQ6.5 ->CTEQ6.6->CT09->CT10
  - NNPDF->NNPDF2.0

gluon dominates at low x

Figure 27. The CTEQ6.1 parton distribution functions evaluated at a Q of 10 GeV.

Global fits

- With the DGLAP equations, we know how to evolve pdf's from a starting scale Q_0 to any higher scale
  - remember the divergences from the initial state that we absorbed into the pdfs
- …but we can't calculate what the pdf's are ab initio
  - one of the goals of lattice QCD
- We have to determine them from a global fit to data
  - factorization theorem tells us that pdf's determined for one process are applicable to another

- So what do we need
  - a value of Q_0 (1.3 GeV for CTEQ, 1 GeV for MSTW) lower than the data used in the fit (or any prediction)
  - a parametrization for the pdf's
  - a scheme for the pdf's
  - hard-scattering calculations at the order being considered in the fit
  - pdf evolution at the order being considered in the fit
  - a world average value for α_s
  - a lot of data
    - with appropriate kinematic cuts
  - a treatment of the errors for the experimental data
  - MINUIT

Back to global fits

- Parametrization: initial form
  - $f(x) \sim x^{\alpha}(1-x)^{\beta}$
  - estimate β from quark counting rules
    - ▲ $\beta = 2n_s - 1$ with n_s being the minimum number of spectator quarks
    - ▲ so for valence quarks in a proton (qqq), $n_s = 2$, $\beta = 3$
    - ▲ for gluon in a proton (qqqg), $n_s = 3$, $\beta = 5$
    - ▲ for anti-quarks in a proton (qqqqqbar), $n_s = 4$, $\beta = 7$
  - estimate α from Regge arguments
    - ▲ gluons and anti-quarks have $\alpha \sim -1$ while valence quarks have $\alpha \sim = 1/2$
  - but at what Q value are these arguments valid?

- What do we know?
1. we know that the sum of the momentum of all partons in the proton is 1 (but not for modified LO fits)
2. we know the sum of valence quarks is 3
   - and 2 of them are up quarks and 1 of them is a down quark
   - we know that the net number of anti-quarks is 0, but what about dbar=ubar
3. we know that the net number of strange quarks (charm quarks/ bottom quarks) in the proton is 0
   - but we don't know if s=sbar locally

This already puts a lot of restrictions on the pdf's

Parametrizations

- That simple parametrization worked for early fits, where the data was not very precise (nor very abundant), but it does not work for modern global fits, where a more flexible form is needed
  - the simple ansatz can be dangerous in that it can (falsely) tie together low x and high x behavior (other than by momentum sum rule)
- In order to more finely tune parametrization,usually multiply simple form by a polynomial in x or some more complicated function

- CTEQ uses for the quark and gluon distributions (CTEQ6.6)

$$f(x) = x^{(a_1-1)}(1-x)^{a_2} e^{a_3 x}[1+e^{a_4}x]^{a_5}$$

- For the ratio of dbar/ubar

$$\frac{\bar{d}}{\bar{u}} = e^{a_1} x^{(a_2-1)}(1-x)^{a_3} + (1+a_4 x)(1-x)^{a_5}$$

- How do we know this is flexible enough?
  - data is well-described (χ^2/dof ~1 for a NLO fit)
  - adding more parameters just results in those parameters being unconstrained
  - but there is some remaining bias
  - note that with this form, the pdf's are positive definite (they don't have to be)

Orders and Schemes

- Fits are available at
  - ◆ LO
    - ▲ CTEQ6L or CTEQ6L1
      - – 1 loop or 2 loop α_s
    - ▲ in common use with parton shower Monte Carlos
    - ▲ poor fit to data due to deficiencies of LO ME's
  - ◆ LO*
    - ▲ better for parton shower Monte Carlos
  - ◆ NLO
    - ▲ CTEQ6.1,CTEQ6.6,CT09
    - ▲ precision level: error pdf's defined at this order
  - ◆ NNLO
    - ▲ more accurate but not all processes known

- At NLO and NNLO, one needs to specify a scheme or convention for subtracting the divergent terms
- Basically the scheme specifies how much of the finite corrections to subtract along with the divergent pieces
  - ◆ most widely used is the modified minimal subtraction scheme (or MSbar)
  - ◆ used with dimensional regularization: subtract the pole terms and accompanying log 4π and Euler constant terms

$$\sigma_{real+virt} = \frac{\alpha_s}{2\pi} C_F \left(\frac{\mu^2}{Q^2}\right)^\varepsilon c_\Gamma \left[\left(\frac{2\pi^2}{3} - 6\right)\delta(1-z) - \frac{2}{\varepsilon} P_{qq}(z) - 2(1-z) + 4(1+z^2)\left[\frac{\ln(1-z)}{1-z}\right]_+ - 2\frac{1+z^2}{1-z}\ln z \right]$$

  - ◆ also may find pdf's in DIS scheme, where full order α_s correction for F_2 in DIS absorbed into quark pdf's

Scales and Masses

- Processes used in global fits are characterized by a single large scale
  - DIS-Q^2
  - lepton pair production-M^2
  - vector boson production-M_V^2
  - jet production-p_T^{jet}
- By choosing the factorization and renormalization scales to be of the same order as the characteristic scale
  - can avoid some large logarithms in the hard scattering cross section
  - some large logarithms in running coupling and pdf's are resummed

- Different treatment of quark masses and thresholds
  - fixed flavor number scheme (FFNS)
  - variable flavor number scheme (VFNS)
    - zero mass variable flavor number scheme (ZM-VFNS)
    - general mass variable flavor number scheme (GM-VFNS)

Data sets used in global fits (CTEQ6.6)

1. BCDMS F_2^{proton} (339 data points)
2. BCDMS $F_2^{deuteron}$ (251 data points)
3. NMC F_2 (201 data points)
4. NMC F_2^d/F_2^p (123 data points)
5. F_2(CDHSW) (85 data points)
6. F_3(CDHSW) (96 data points)
7. CCFR F_2 (69 data points)
8. CCFR F_3 (86 data points)
9. H1 NC e^-p (126 data points; 1998-98 reduced cross section)
10. H1 NC e^-p (13 data points; high y analysis)
11. H1 NC e^+p (115 data points; reduced cross section 1996-97)
12. H1 NC e^+p (147 data points; reduced cross section; 1999-00)
13. ZEUS NC e^-p (92 data points; 1998-99)
14. ZEUS NC e^+p (227 data points; 1996-97)
15. ZEUS NC e^+p (90 data points; 1999-00)
16. H1 F_2^c e^+p (8 data points;1996-97)
17. H1 $R\sigma^c$ for ccbar e^+p (10 data points;1996-97)
18. H1 R_σ^b for bbbar e^+p (10 data points; 1999-00)
19. ZEUS F_2^c e^+p (18 data points; 1996/97)
20. ZEUS F_2^C $e+p$ (27 data points; 1998/00)
21. H1 CC e^-p (28 data points; 1998-99)
22. H1 CC e^+p (25 data points; 1994-97)
23. H1 CC e^+p (28 data points; 1999-00)
24. ZEUS CC e^-p (26 data points; 1998-99)
25. ZEUS CC e^+p (29 data points; 1994-97)
26. ZEUS CC e^+p (30 data points; 1999-00)
27. NuTev neutrino dimuon cross section (38 data points)
28. NuTev anti-neutrino dimuon cross section (33 data points)
29. CCFR neutrino dimuon cross section (40 data points)
30. CCFR anti-neutrino cross section (38 data points)
31. E605 dimuon (199 data points)
32. E866 dimuon (13 data points)
33. Lepton asymmetry from CDF (11 data points)
34. CDF Run 1B jet cross section (33 data points)
35. D0 Run 1B jet cross section (90 data points)

- 2794 data points from DIS, DY, jet production
- All with (correlated) systematic errors that must be treated correctly in the fit
- Note that DIS is the 800 pound gorilla of the global fit with many data points and small statistical and systematic errors
  - and fixed target DIS data still have a significant impact on the global fitting, even with an abundance of HERA data
- To avoid non-perturbative effects, kinematic cuts on placed on the DIS data
  - $Q^2 > 5$ GeV^2
  - $W^2 (= m^2 + Q^2(1-x)/x) > 12.25$ GeV^2

Influence of data in global fit

- **Charged lepton DIS**

$$F_2(x,Q^2) = x \sum_i e_i^2 [q_i(x,Q^2) + \overline{q}_i(x,Q^2)]$$

- each flavor weighted by its squared charge

- quarks and anti-quarks enter together

- gluon doesn't enter, in lowest order, but does enter into the structure functions at NLO

- also enters through mixing in evolution equations so gluon contributes to the change of the structure functions as Q^2 increases

- at low values of x

$$Q^2 \frac{dF_2}{dQ^2} \approx \frac{\alpha_s}{2\pi} \sum_i e_i^2 \int_x^1 \frac{dy}{y} P_{qg}(y) G(\frac{x}{y},Q^2)$$

- Q^2 dependence at small x is driven directly by gluon pdf

- At low x, structure functions increase with Q^2; at high x decrease
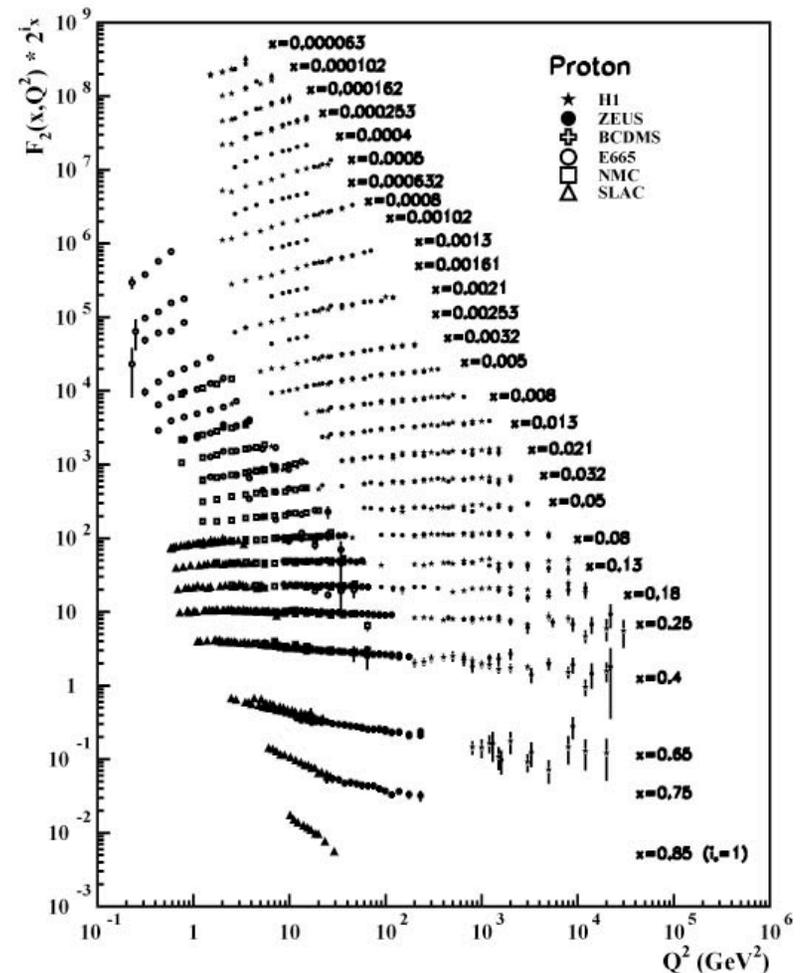
Influence of data in global fit

Neutrino DIS

$$F_2(x,Q^2) = x\sum_i [q_i(x,Q^2) + \bar{q}_i(x,Q^2)]$$

$$xF_3(x,Q^2) = x\sum_i [q_i(x,Q^2) - \bar{q}_i(x,Q^2)]$$

- additional (parity-violating) structure function allows the separation of quarks and antiquarks but not a complete flavor separation

- caveat: neutrino observables usually obtained using nuclear targets so there is added question of nuclear corrections

Some observations from DIS

- DIS data provide strong constraints on the u and d distributions over the full range of x covered by the data

- The combination 4*ubar + dbar is well-constrained at small x

- The gluon is constrained at low values of x by the slope of the Q^2 dependence of F_2
    - momentum sum rule connects low x and high x behavior, but loosely

Inclusive jets and global fits

- We don't have many handles on the high x gluon distribution in the global pdf fits
- Best handle is provided by the inclusive jet cross section from the Tevatron

Figure 56. The subprocess contributions to inclusive jet production at the Tevatron for the CTEQ5M and CTEQ6M pdfs. The impact of the larger larger gluon at high x for CTEQ6 is evident.

- At high E_T (high x), gq is subdominant, but there's a great deal of freedom/uncertainty on the high x gluon distribution
  - about 42% of the proton's momentum is carried by gluons, and most of that momentum is at low x
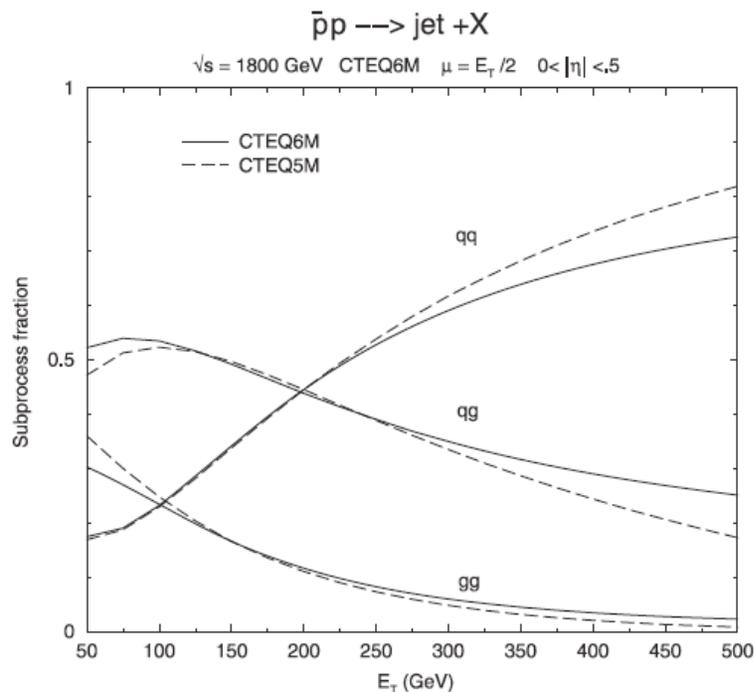
X Bin	Momentum fraction
10^{-4} to 10^{-3}	0.6%
10^{-3} to 0.01	3%
0.01 to 0.1	16%
0.1 to 0.2	10%
0.2 to 0.3	6%
0.3 to 0.5	5%
0.5 to 1.0	1%

TABLE I. The momentum fraction carried by gluons in a a given x bin at a Q value of 5 GeV.

- The inclusion of the CDF/D0 inclusive jet cross sections from Run 1 boosted the high x gluon distribution and thus the predictions for the high E_T jet cross sections
  - The high x gluon has decreased due to influence of the Run 2 jet data

Global fitting: best fit

- Using our 2794 data points, we do our global fit by performing a χ^2 minimization
  - where D_i are the data points and T_i are the theoretical predictions; we allow for a normalization shift f_N for each experimental data set
    - but we provide a quadratic penalty for any normalization shift
  - where there are k systematic errors β for each data point in a particular data set
    - and where we allow the data points to be shifted by the systematic errors with the shifts given by the s_j parameters
    - but we give a quadratic penalty for non-zero values of the shifts s_j
  - where σ_i is the statistical error for data point i

- For each data set, we calculate

$$\chi^2 = \sum_i \frac{\left[\left(f_N D_i - \sum_{j=1}^{k} \beta_{ij} s_j\right) - T_i\right]^2}{\sigma_i^2} + \sum_{j=1}^{k} s_j^2$$

- For a set of theory parameters it is possible to analytically solve for the shifts s_j, and therefore, continually update them as the fit proceeds

- To make matters more complicated, we may give additional weights to some experiments due to the utility of the data in those experiments (i.e. NA-51), so we adjust the χ^2 to be

$$\chi^2 = \sum_k w_k \chi_k^2 + \sum_k w_{N,k} \left[\frac{1 - f_N}{\sigma_N^{norm}}\right]^2$$

- where w_k is a weight given to the experimental data and $w_{N,k}$ is a weight given to the normalization

Minimization and errors

- Free parameters in the fit are parameters for quark and gluon distributions

$$f(x) = x^{(a_1-1)}(1-x)^{a_2} e^{a_3 x}[1 + e^{a_4} x]^{a_5}$$

- Too many parameters to allow all to remain free
  - some are fixed at reasonable values or determined by sum rules
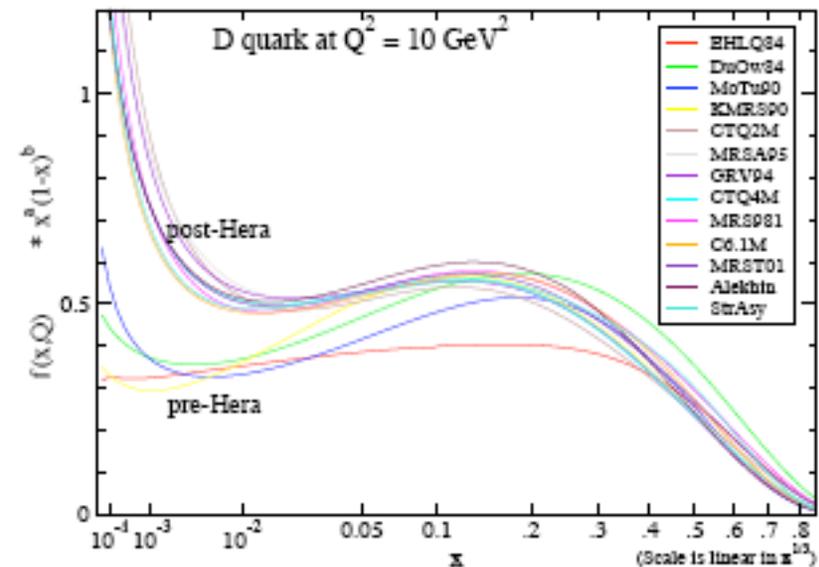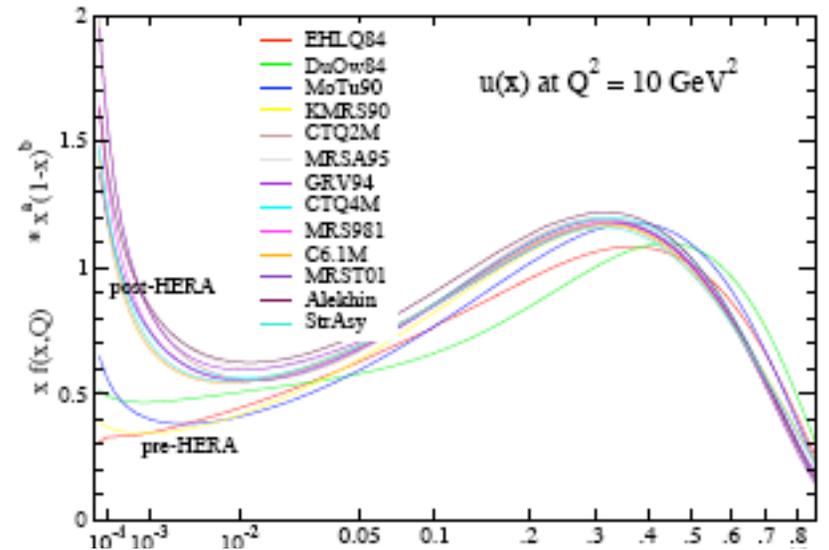- 20 free parameters for CTEQ6.1, 22 for CTEQ6.6,24 for CT09, 26 for CT10

- Result is a global χ^2/dof on the order of 1
  - for a NLO fit
  - worse for a LO fit, since the LO pdf's can not make up for the deficiencies in the LO matrix elements

CTEQ6M PDFs
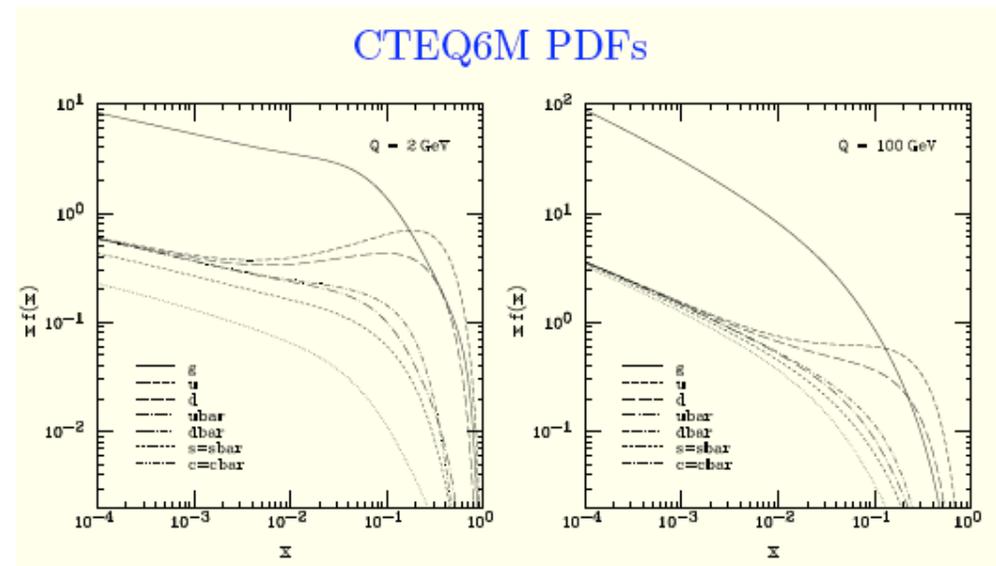
PDF Errors: old way

- Make plots of lots of pdf's (no matter how old) and take spread as a measure of the error
- Can either underestimate or overestimate the error
- Review sources of uncertainty on pdf's
  - data set choice
  - kinematic cuts
  - parametrization choices
  - treatment of heavy quarks
  - order of perturbation theory
  - errors on the data
- There are now more sophisticated techniques to deal with at least the errors due to the experimental data uncertainties

PDF Errors: new way

- So we have optimal values (minimum χ^2) for the d=20 (22 for CTEQ6.6, 26 for CT10) free pdf parameters in the global fit
  - $\{a_\mu\}, \mu=1,\ldots d$
- Varying any of the free parameters from its optimal value will increase the χ^2
- It's much easier to work in an orthonormal eigenvector space determined by diagonalizing the Hessian matrix, determined in the fitting process

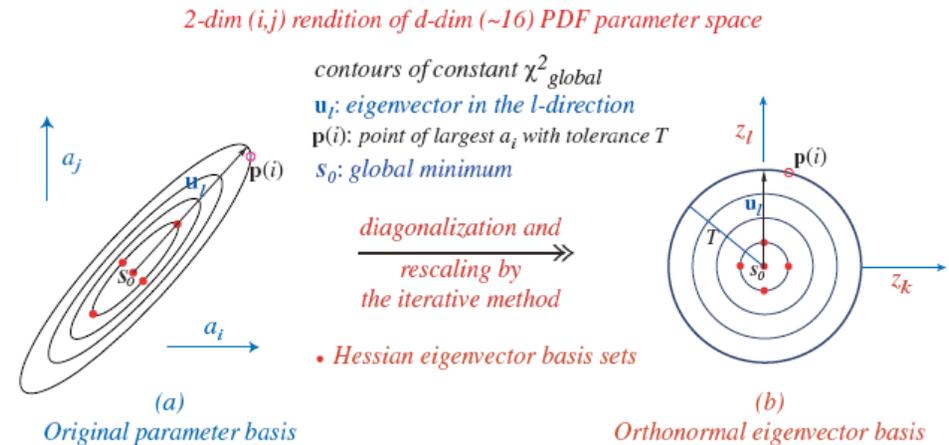$$H_{uv} = \frac{1}{2}\frac{\partial \chi^2}{\partial a_\mu \partial a_\nu}$$

2-dim (i,j) rendition of d-dim (~16) PDF parameter space

contours of constant χ^2_{global}

$\mathbf{u}_l$: eigenvector in the l-direction

$\mathbf{p}(i)$: point of largest a_i with tolerance T

s_0: global minimum

diagonalization and rescaling by the iterative method

• Hessian eigenvector basis sets

(a)
Original parameter basis
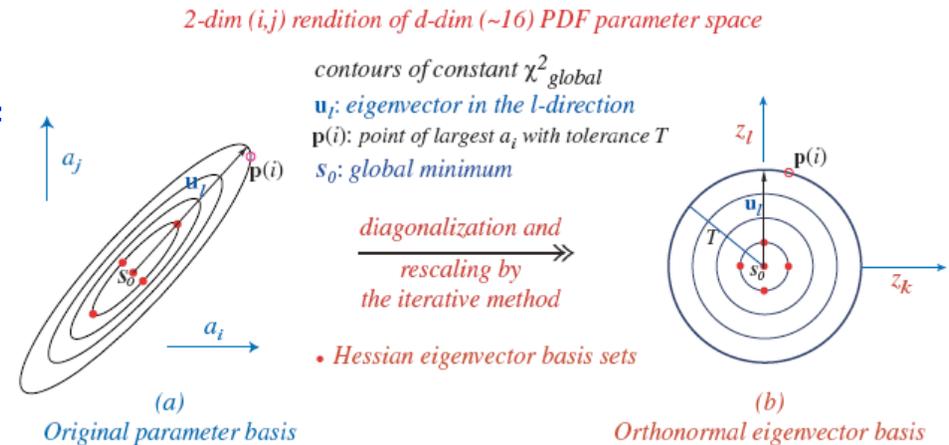
(b)
Orthonormal eigenvector basis

Figure 28. A schematic representation of the transformation from the pdf parameter basis to the orthonormal eigenvector basis.

To estimate the error on an observable X(a), due to the experimental uncertainties of the data used in the fit, we use the *Master Formula*

$$(\Delta X)^2 = \Delta \chi^2 \sum_{\mu,\nu} \frac{\partial X}{\partial a_\mu}\left(H^{-1}\right)_{\mu\nu} \frac{\partial X}{\partial a_\nu}$$

PDF Errors: new way

- Recap: 20 (22,26) eigenvectors with the eigenvalues having a range of >1E6

- Largest eigenvalues (low number eigenvectors) correspond to best determined directions; smallest eigenvalues (high number eigenvectors) correspond to worst determined directions

- Easiest to use Master Formula in eigenvector basis

$$\Delta X^+_{max} = \sqrt{\sum_{i=1}^{N} [\max(X_i^+ - X_0, X_i^- - X_0, 0)]^2},$$

$$\Delta X^-_{max} = \sqrt{\sum_{i=1}^{N} [\max(X_0 - X_i^+, X_0 - X_i^-, 0)]^2}.$$

2-dim (i,j) rendition of d-dim (~16) PDF parameter space

contours of constant χ^2_{global}
$\mathbf{u}_l$: eigenvector in the l-direction
$\mathbf{p}(i)$: point of largest a_i with tolerance T
s_0: global minimum

diagonalization and rescaling by the iterative method

• Hessian eigenvector basis sets

(a) Original parameter basis

(b) Orthonormal eigenvector basis

Figure 28. A schematic representation of the transformation from the pdf parameter basis to the orthonormal eigenvector basis.

To estimate the error on an observable X(a), from the experimental errors, we use the *Master Formula*

$$(\Delta X)^2 = \Delta \chi^2 \sum_{\mu,\nu} \frac{\partial X}{\partial a_\mu} \left(H^{-1}\right)_{\mu\nu} \frac{\partial X}{\partial a_\nu}$$

where X_i^+ and X_i^- are the values for the observable X when traversing a distance corresponding to the tolerance T(=sqrt($\Delta\chi^2$)) along the ith direction

PDF Errors: new way

- What is the tolerance T?

- This is one of the most controversial questions in global pdf fitting?

- We have 2794 data points in the CTEQ6.6 data set (on order of 2000 for CTEQ6.1)

- Technically speaking, a 1-sigma error corresponds to a tolerance $T(=\sqrt{\Delta\chi^2})=1$

- This results in far too small an uncertainty from the global fit

  - with data from a variety of processes from a variety of experiments from a variety of accelerators

- For CTEQ6.1/6.6, we chose a $\Delta\chi^2$ of 100 to correspond to a 90% CL limit

  - with an appropriate scaling for the larger data set for CTEQ6.6

- In the past, MSTW has chosen a $\Delta\chi^2$ of 50 for the same limit so CTEQ errors were larger than MSTW errors

$$\Delta X_{\max}^+ = \sqrt{\sum_{i=1}^{N}[\max(X_i^+ - X_0, X_i^- - X_0, 0)]^2},$$

$$\Delta X_{\max}^- = \sqrt{\sum_{i=1}^{N}[\max(X_0 - X_i^+, X_0 - X_i^-, 0)]^2}.$$
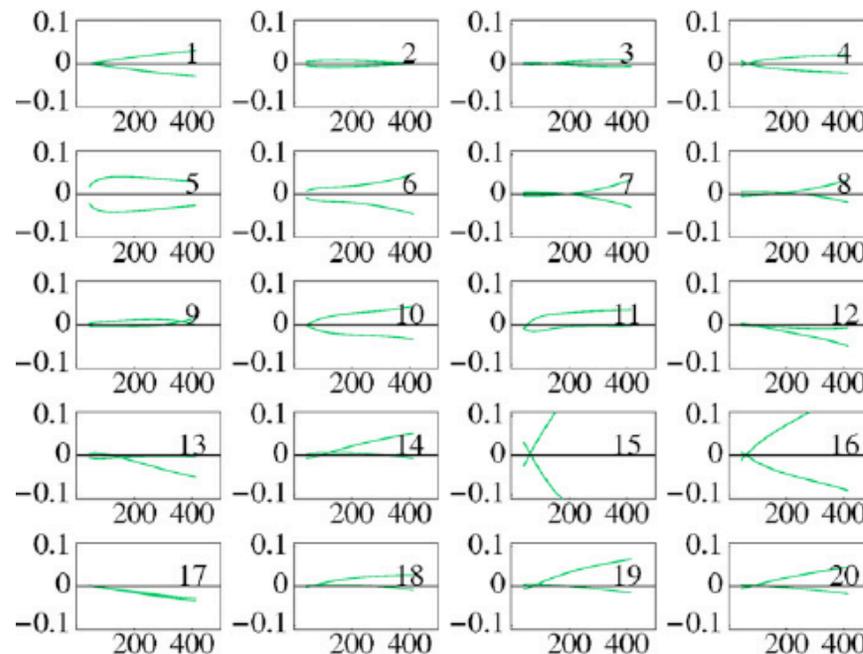
Figure 29. The pdf errors for the CDF inclusive jet cross section in Run 1 for the 20 different eigenvector directions. The vertical axes show the fractional deviation from the central prediction and the horizontal axes the jet transverse momentum in GeV.

Parametrization bias

- It's been shown by Jon Pumplin (**arXiv: 0909.5176)** that a large part of the need for a large value of $\Delta\chi^2$ is because of remaining parameterization biases present even with a very flexible parameterization

- Comparisons with NNPDF (which has less bias) even more important

What do the eigenvectors *mean*?

- Each eigenvector corresponds to a linear combination of all 20 (22,24) pdf parameters, so in general each eigenvector doesn't mean anything?
- However, with 20 (22,24,26) dimensions, often eigenvectors will have a large component from a particular direction
- Take eigenvector 1 (for CTEQ6.1); error pdf's 1 and 2
- It has a large component sensitive to the small x behavior of the u quark valence distribution
- Not surprising since this is the best determined direction

Sets	Shape Parameter	Component
1, 2	BP(2, 1)	0.057911
1, 2	BP(2, 2)	−0.022688
1, 2	BP(2, 3)	0.015496
1, 2	BP(2, 4)	0.035277
1, 2	BP(2, 5)	frozen
1, 2	BP(1, 1)	0.888833
1, 2	BP(1, 2)	−0.161942
1, 2	BP(1, 3)	0.118204
1, 2	BP(1, 4)	0.268405
1, 2	BP(1, 5)	0.276392
1, 2	BP(0, 1)	0.038555
1, 2	BP(0, 2)	−0.006610
1, 2	BP(0, 3)	frozen
1, 2	BP(0, 4)	−0.017717
1, 2	BP(0, 5)	frozen
1, 2	BP(−1, 1)	−0.007668
1, 2	BP(−1, 2)	0.012745
1, 2	BP(−1, 3)	0.001851
1, 2	BP(−1, 4)	frozen
1, 2	BP(−1, 5)	0.001004
1, 2	BP(−2, 1)	0.117517
1, 2	BP(−2, 2)	−0.008357
1, 2	BP(−2, 3)	0.006504
1, 2	BP(−2, 4)	frozen
1, 2	BP(−2, 5)	frozen

What do the eigenvectors *mean*?

- Take eigenvector 8 (for CTEQ6.1); error pdf's 15 and 16

- No particular direction stands out

Sets	Shape Parameter	Component
15, 16	BP(2, 1)	0.196388
15, 16	BP(2, 2)	0.387704
15, 16	BP(2, 3)	-0.226202
15, 16	BP(2, 4)	-0.411440
15, 16	BP(2, 5)	frozen
15, 16	BP(1, 1)	-0.193195
15, 16	BP(1, 2)	0.356604
15, 16	BP(1, 3)	0.018064
15, 16	BP(1, 4)	0.468888
15, 16	BP(1, 5)	0.376180
15, 16	BP(0, 1)	0.016734
15, 16	BP(0, 2)	-0.026136
15, 16	BP(0, 3)	frozen
15, 16	BP(0, 4)	-0.016537
15, 16	BP(0, 5)	frozen
15, 16	BP(-1, 1)	-0.176169
15, 16	BP(-1, 2)	0.136337
15, 16	BP(-1, 3)	0.074431
15, 16	BP(-1, 4)	frozen
15, 16	BP(-1, 5)	-0.030040
15, 16	BP(-2, 1)	-0.014533
15, 16	BP(-2, 2)	-0.067391
15, 16	BP(-2, 3)	0.049273
15, 16	BP(-2, 4)	frozen
15, 16	BP(-2, 5)	frozen

What do the eigenvectors *mean*?

- Take eigenvector 15 (for CTEQ6.1); error pdf's 29 and 30
- Probes high x gluon distribution

creates largest uncertainty for high p_T jet cross sections at both the Tevatron and LHC

```
29, 30    BP(  2, 1)     0.012701
29, 30    BP(  2, 2)    -0.162018
29, 30    BP(  2, 3)     0.018666
29, 30    BP(  2, 4)    -0.111238
29, 30    BP(  2, 5)       frozen
29, 30    BP(  1, 1)    -0.003049
29, 30    BP(  1, 2)    -0.001074
29, 30    BP(  1, 3)    -0.034151
29, 30    BP(  1, 4)    -0.005735
29, 30    BP(  1, 5)     0.032812
29, 30    BP(  0, 1)    -0.045923
29, 30    BP(  0, 2)     0.873418
29, 30    BP(  0, 3)       frozen
29, 30    BP(  0, 4)    -0.241822
29, 30    BP(  0, 5)       frozen
29, 30    BP( -1, 1)    -0.071419
29, 30    BP( -1, 2)    -0.067488
29, 30    BP( -1, 3)     0.100283
29, 30    BP( -1, 4)       frozen
29, 30    BP( -1, 5)     0.179551
29, 30    BP( -2, 1)    -0.009441
29, 30    BP( -2, 2)    -0.196100
29, 30    BP( -2, 3)     0.211281
29, 30    BP( -2, 4)       frozen
29, 30    BP( -2, 5)       frozen
```
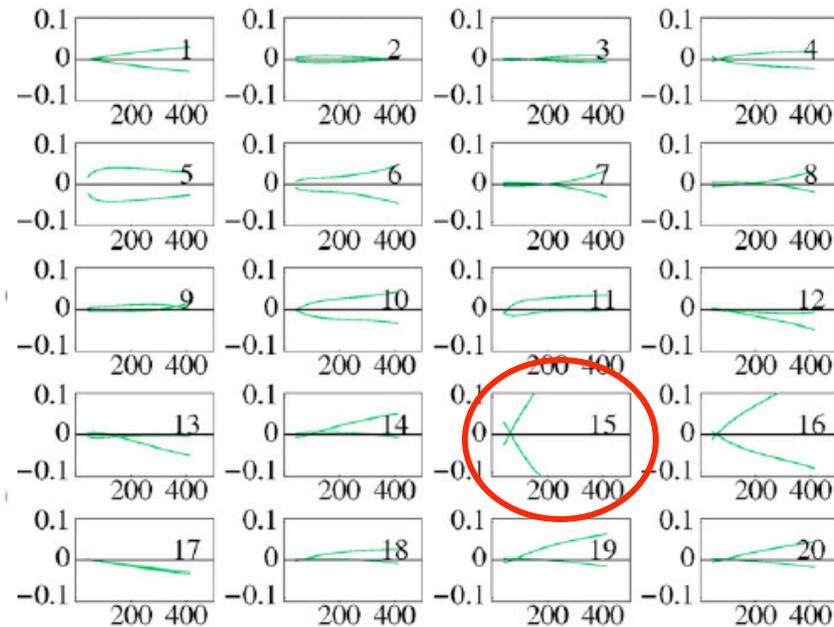

Figure 29. The pdf errors for the CDF inclusive jet cross section in Run 1 for the 20 different eigenvector directions. The vertical axes show the fractional deviation from the central prediction and the horizontal axes the jet transverse momentum in GeV.

Aside: PDF re-weighting

- Any physical cross section at a hadron-hadron collider depends on the product of the two pdf's for the partons participating in the collision convoluted with the hard partonic cross section

$$\sigma_{AB} = \int dx_a dx_b \; f_{a/A}(x_a, Q^2) f_{b/B}(x_b, Q^2) \; \hat{\sigma}_{ab \to X}$$

- Nominally, if one wants to evaluate the pdf uncertainty for a cross section, this convolution should be carried out 41 times (for CTEQ6.1); once for the central pdf and 40 times for the error pdf's

f^i is the error pdf and f^0 the central pdf

$$\frac{f^i_{a/A}(x_a, Q^2) f^i_{b/B}(x_b, Q^2)}{f^0_{a/A}(x_a, Q^2) f^0_{b/B}(x_b, Q^2)}$$

- However, the partonic cross section is not changing, only the product of the pdf's

- So one can evaluate the full cross section for one pdf (the central pdf) and then evaluate the pdf uncertainty for a particular cross section by taking the ratio of the product of the pdf's (the pdf luminosity) for each of the error pdf's compared to the central pdf's

This works exactly for fixed order calculations and works well enough (see later) for parton shower Monte carlo calculations.

Most experiments now have code to easily do this…
and many programs will do it for you (MCFM)

A very useful tool

Allows easy calculation and comparison of pdf's

Let's try it out

Up and down quarks dominate at high x, gluon at low x.
As Q^2 increases, note the growth of the gluon distribution, and to a lesser extent the sea quark distributions.
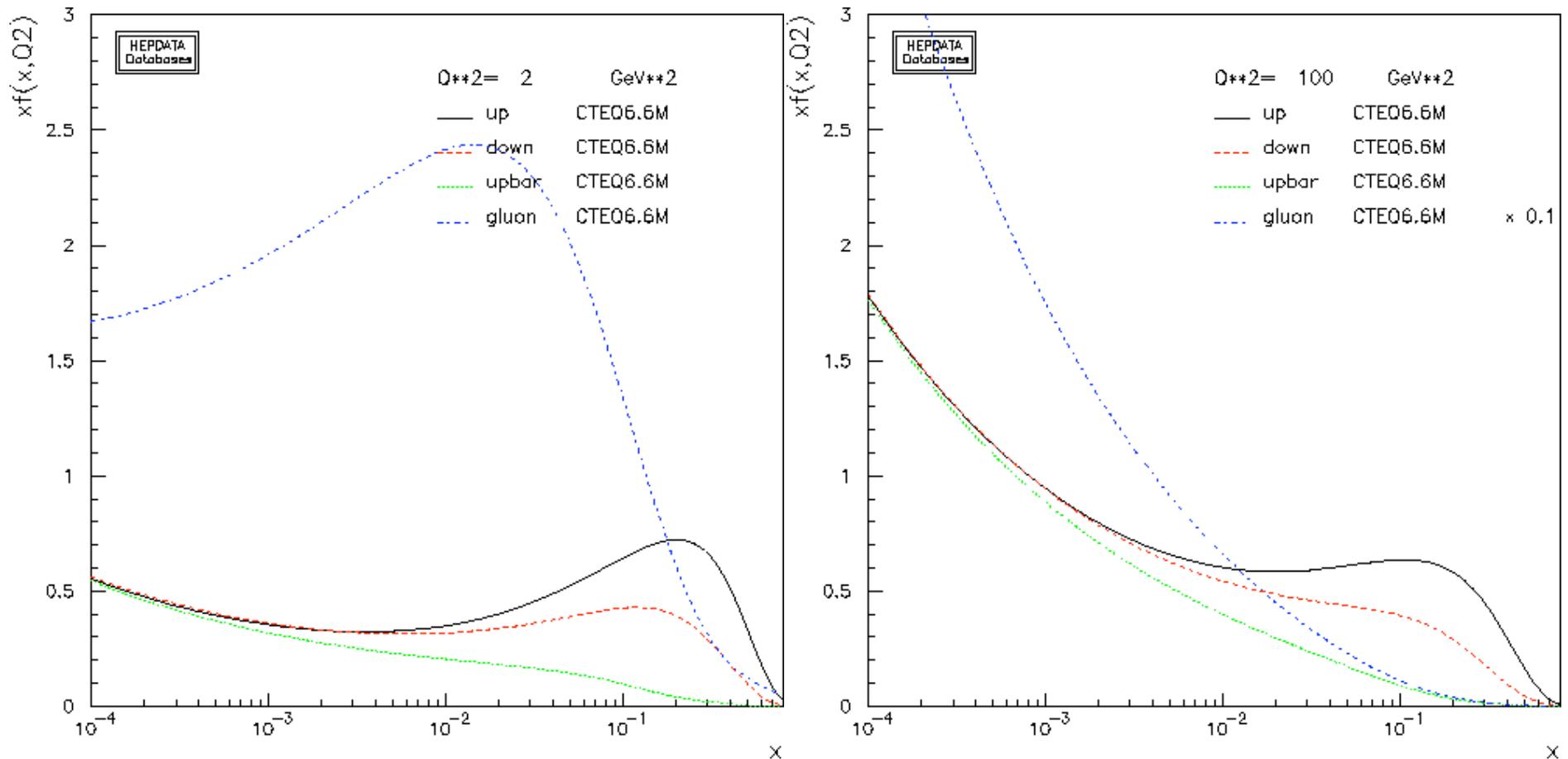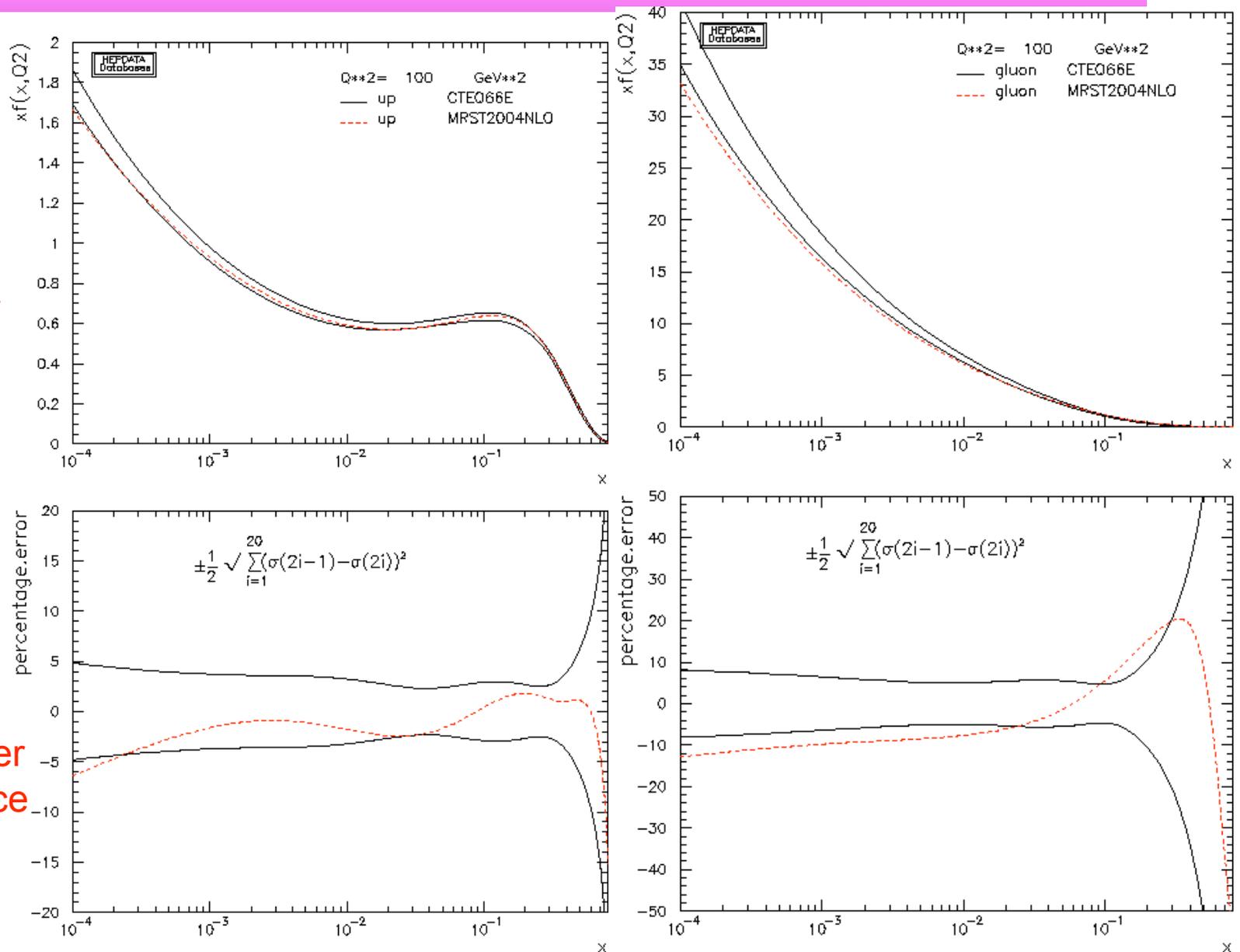
Uncertainties
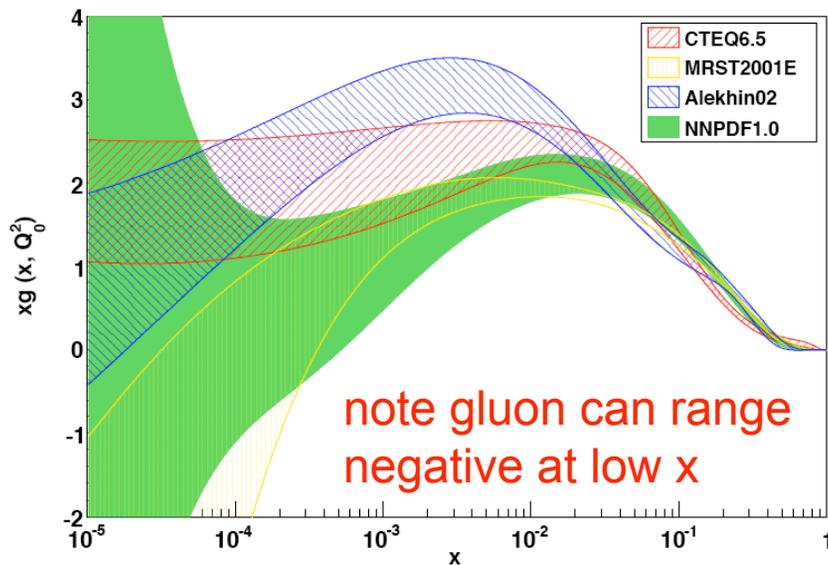

uncertainties get large at high x

uncertainty for gluon larger than that for quarks

pdf's from one group don't necessarily fall into uncertainty band of another …would be nice if they did
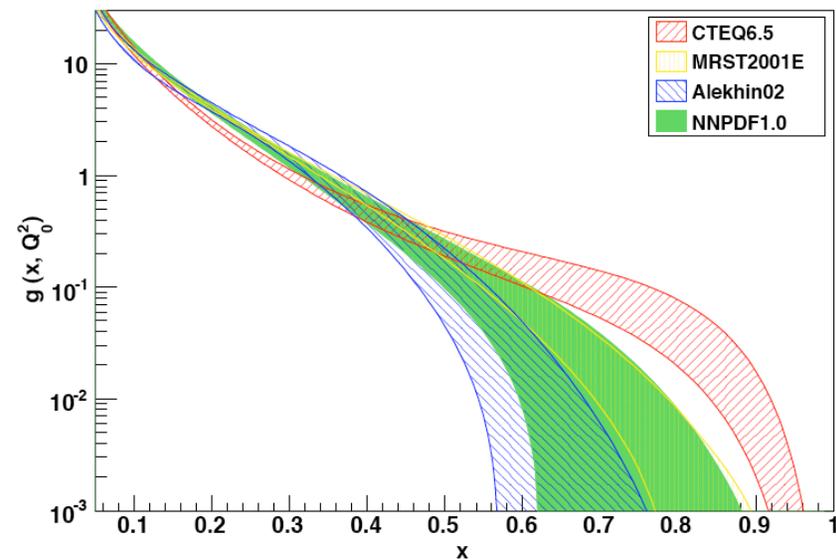
Uncertainties and parametrizations

- Beware of extrapolations to x values smaller than data available in the fits, especially at low Q^2

- Parameterization may artificially reduce the apparent size of the uncertainties

- Compare for example uncertainty for the gluon at low x from the recent neural net global fit to global fits using a parametrization

note gluon can range negative at low x

Q^2=2 GeV^2

Correlations

- Consider a cross section X(a)
- i^{th} component of gradient of X is

$$\frac{\partial X}{\partial a_i} \equiv \partial_i X = \frac{1}{2}(X_i^{(+)} - X_i^{(-)})$$

- Now take 2 cross sections X and Y
  - or one or both can be pdf's
- Consider the projection of gradients of X and Y onto a circle of radius 1 in the plane of the gradients in the parton parameter space
- The circle maps onto an ellipse in the XY plane
- The angle ϕ between the gradients of X and Y is given by

$$\cos \varphi = \frac{\vec{\nabla} X \cdot \vec{\nabla} Y}{\Delta X \Delta Y} = \frac{1}{4 \Delta X \, \Delta Y} \sum_{i=1}^{N} \left(X_i^{(+)} - X_i^{(-)} \right) \left(Y_i^{(+)} - Y_i^{(-)} \right)$$

- The ellipse itself is given by

$$\left(\frac{\delta X}{\Delta X} \right)^2 + \left(\frac{\delta Y}{\Delta Y} \right)^2 - 2 \left(\frac{\delta X}{\Delta X} \right) \left(\frac{\delta Y}{\Delta Y} \right) \cos \varphi = \sin^2 \varphi$$

2-dim (i,j) rendition of d-dim (~16) PDF parameter space

contours of constant χ^2_{global}
$\mathbf{u}_l$: eigenvector in the l-direction
$\mathbf{p}(i)$: point of largest a_i with tolerance T
s_0: global minimum

diagonalization and rescaling by the iterative method

• Hessian eigenvector basis sets

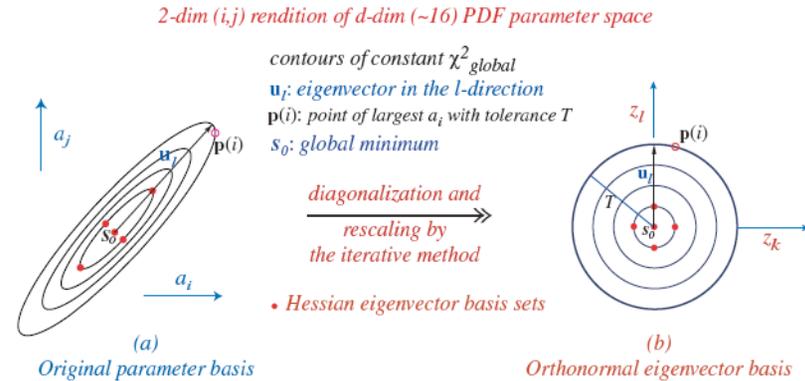(a) Original parameter basis

(b) Orthonormal eigenvector basis

Figure 28. A schematic representation of the transformation from the pdf parameter basis to the orthonormal eigenvector basis.

- If two cross sections/pdf's are very correlated, then $\cos\phi \sim 1$
- …uncorrelated, then $\cos\phi \sim 0$
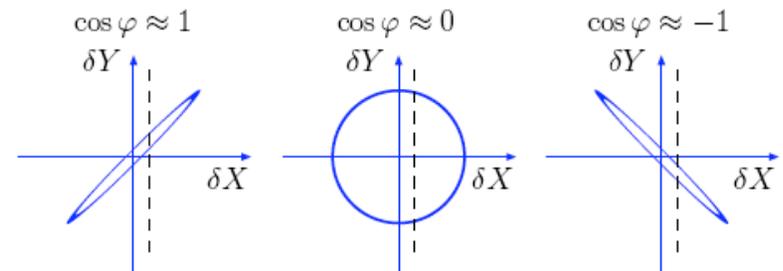- …anti-correlated, then $\cos\phi \sim -1$

Figure 1: Dependence on the correlation ellipse formed in the $\Delta X - \Delta Y$ plane on the value of the correlation cosine $\cos \varphi$.

Correlations

- Consider a cross section X(a)
- i^{th} component of gradient of X is

$$\frac{\partial X}{\partial a_i} \equiv \partial_i X = \frac{1}{2}(X_i^{(+)} - X_i^{(-)})$$

- Now take 2 cross sections X and Y
  - or one or both can be pdf's
- Consider the projection of gradients of X and Y onto a circle of radius 1 in the plane of the gradients in the parton parameter space
- The circle maps onto an ellipse in the XY plane
- The angle ϕ between the gradients of X and Y is given by

$$\cos \varphi = \frac{\vec{\nabla} X \cdot \vec{\nabla} Y}{\Delta X \Delta Y} = \frac{1}{4 \Delta X \, \Delta Y} \sum_{i=1}^{N} \left(X_i^{(+)} - X_i^{(-)} \right) \left(Y_i^{(+)} - Y_i^{(-)} \right)$$

- The ellipse itself is given by

$$\left(\frac{\delta X}{\Delta X} \right)^2 + \left(\frac{\delta Y}{\Delta Y} \right)^2 - 2 \left(\frac{\delta X}{\Delta X} \right) \left(\frac{\delta Y}{\Delta Y} \right) \cos \varphi = \sin^2 \varphi$$

2-dim (i,j) rendition of d-dim (~16) PDF parameter space

contours of constant χ^2_{global}
$\mathbf{u}_l$: eigenvector in the l-direction
$\mathbf{p}(i)$: point of largest a_i with tolerance T
s_0: global minimum

diagonalization and
rescaling by
the iterative method

- Hessian eigenvector basis sets

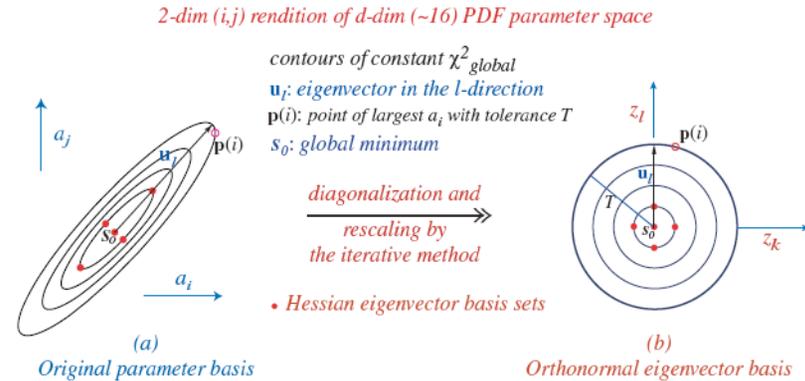(a) Original parameter basis

(b) Orthonormal eigenvector basis

Figure 28. A schematic representation of the transformation from the pdf parameter basis to the orthonormal eigenvector basis.

- If two cross sections/pdf's are very correlated, then $\cos\phi \sim 1$
- …uncorrelated, then $\cos\phi \sim 0$
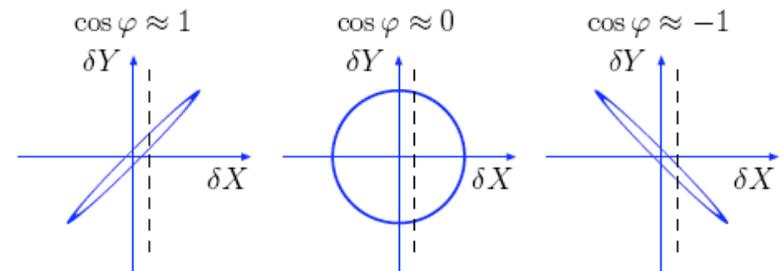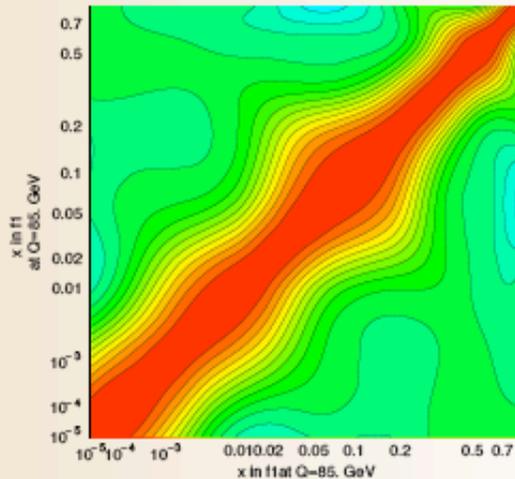- …anti-correlated, then $\cos\phi \sim -1$

Figure 1: Dependence on the correlation ellipse formed in the $\Delta X - \Delta Y$ plane on the value of the correlation cosine $\cos \varphi$.

Correlations between pdf's

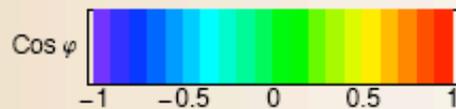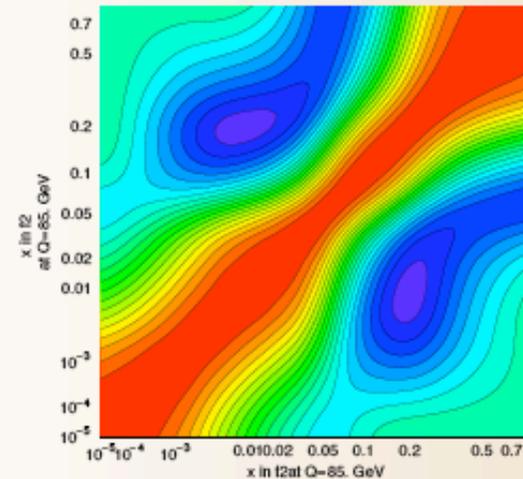**Correlations between $f(x_1, Q)$ and $f(x_2, Q)$ at $Q = 85$ GeV**

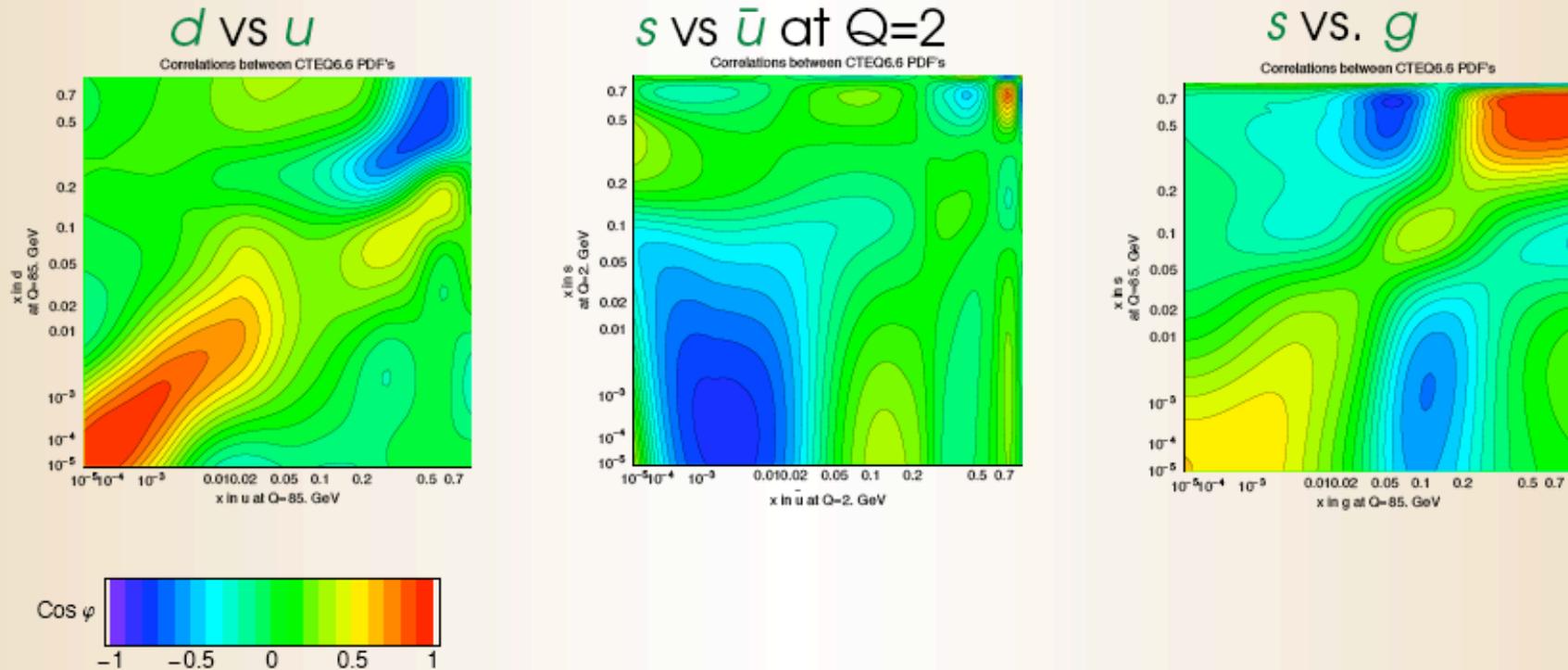$f_1(x_1, Q)$ vs. $f_1(x_2, Q)$

$f_2(x_1, Q)$ vs. $f_2(x_2, Q)$

Can you guess which PDF's these are?

Pavel Nadolsky

Homework assignment: which pdf's and why?

Correlations between $f_1(x_1, Q)$ and $f_2(x_2, Q)$ at $Q = 85$ GeV

Sometimes there is a clear physics reason behind the correlation (e.g., sum rules or assumed Regge-like behavior); sometimes not

α_S uncertainties

- Another uncertainty is that due to the variation in the value of α_s
- MSTW has recently tried to better quantify the uncertainty due to the variation of α_s, by performing global fits over a finer range, taking into account correlations between the values of α_s and the PDF errors
- Procedure is a bit complex

PDF uncertainties given by [1]

$$(\Delta F_{\text{PDF}}^{\alpha_S})_+ = \sqrt{\sum_{k=1}^{n} \left\{ \max \left[F^{\alpha_S}(S_k^+) - F^{\alpha_S}(S_0), \; F^{\alpha_S}(S_k^-) - F^{\alpha_S}(S_0), \; 0 \right] \right\}^2},$$

$$(\Delta F_{\text{PDF}}^{\alpha_S})_- = \sqrt{\sum_{k=1}^{n} \left\{ \max \left[F^{\alpha_S}(S_0) - F^{\alpha_S}(S_k^+), \; F^{\alpha_S}(S_0) - F^{\alpha_S}(S_k^-), \; 0 \right] \right\}^2},$$

for each of the five fixed values of α_S. Then the overall best-fit prediction is $F^{\alpha_S^0}(S_0)$, α_S^0 is the best-fit α_S value, and the overall "PDF+α_S" uncertainties are given by

$$(\Delta F_{\text{PDF}+\alpha_S})_+ = \max_{\alpha_S} \left(\{ F^{\alpha_S}(S_0) + (\Delta F_{\text{PDF}}^{\alpha_S})_+ \} \right) - F^{\alpha_S^0}(S_0),$$

$$(\Delta F_{\text{PDF}+\alpha_S})_- = F^{\alpha_S^0}(S_0) - \min_{\alpha_S} \left(\{ F^{\alpha_S}(S_0) - (\Delta F_{\text{PDF}}^{\alpha_S})_- \} \right).$$

Since this prescription might look quite complicated at first sight, we will give a few concrete examples of its application and consequences in the following subsections.[3]

Higgs cross sections with MSTW 2008 NNLO PDFs
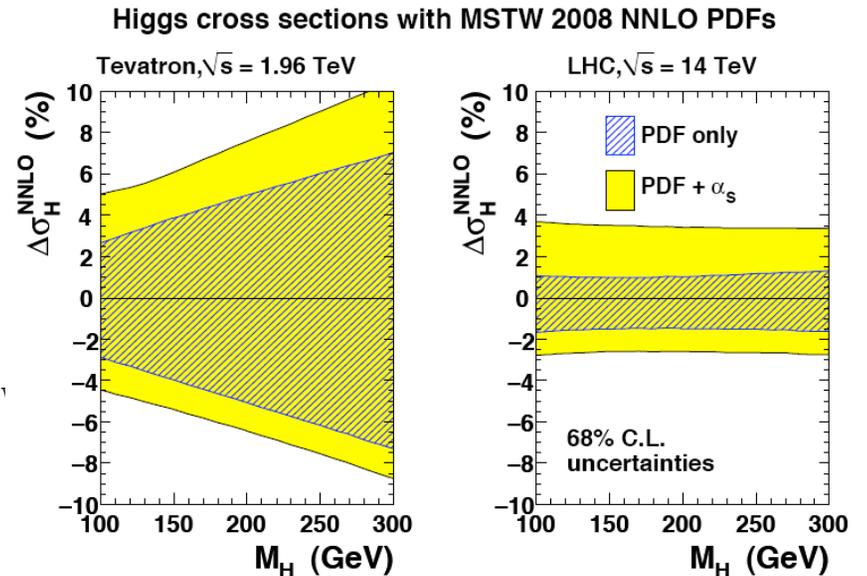
- In many cases, no simple scaling between 68% and 90% CL

$\alpha_s(m_Z)$ and uncertainty: a complication

- Different values of α_s and of its uncertainty are used
- CTEQ and NNPDF use the world average (actually 0.118 for CTEQ and 0.119 for NNPDF), where MSTW2008 uses 0.120, as determined from their best fit

NLO $\alpha_s(M_Z^2)$ values used by different PDF groups

68% C.L. PDF
- ● MSTW08
- ■ CTEQ6.6
- ▲ NNPDF2.0
- ▼ HERAPDF1.0
- ◇ ABKM09
- ✛ GJR08

0.11 0.112 0.114 0.116 0.118 0.12 0.122 0.124 0.126 0.128 0.13
$\alpha_s(M_Z^2)$

G. Watt Mar 26 PDF4LHC meeting
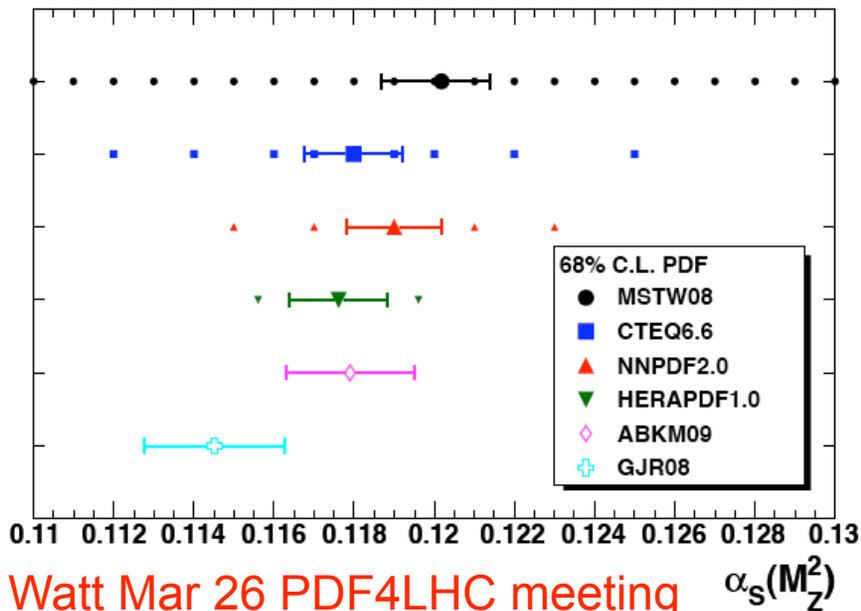
- Latest world average (from Siggi Bethke->PDG)
  - ◆ $\alpha_s(m_Z)$ = 0.1184 +/- 0.0007
- What does the error represent?
  - ◆ Siggi said that only one of the results included in his world average was outside this range
  - ◆ suppose we say that +/-0.002 is a reasonable estimate of the uncertainty

$\alpha_s(m_Z)$ and uncertainty

- Could it be possible for all global PDF groups to use the world average value of α_s in their fits, plus a prescribed 90% range for its uncertainty (if not 0.002, then perhaps another acceptable value)?

- After that, world peace

- For the moment, we try determining uncertainties from α_s over a range of +/- 0.002 from the central value for each PDF group; we also calculate cross sections with a common value of α_s=0.119 for comparison purposes

My recommendation to PDF4LHC/Higgs working group

- Cross sections should be calculated with MSTW2008, CTEQ6.6 and NNPDF

- Upper range of prediction should be given by upper limit of error prediction using prescription for combining α_s uncertainty with error PDFs
  - in quadrature for CTEQ6.6 and NNPDF
  - using eigenvector sets for different values of α_s for MSTW2008
  - (my suggestion) as standard, use 90%CL limits
  - note that this effectively creates a larger α_s uncertainty range

- Ditto for lower limit

- So for a Higgs mass of 120 GeV at 14 TeV, it turns out that the gg cross section lower limit would be defined by the CTEQ6.6 lower limit (PDF+α_s error) and the upper limit defined by the MSTW2008 upper limit (PDF+α_s error)
  - with the difference between the central values primarily due to α_s
  - I'll come back to using the Higgs as an example in the last lecture

- To fully understand similarities/differences of cross sections/uncertainties conduct a benchmarking exercise, to which all groups are invited to participate

- In lecture #5

NNLO addendum

- NNLO is important for some cross sections (as we saw for gg->Higgs)
- Not all processes used for global fits are available at NNLO (inclusive jet production for example)
- Only global fit at NNLO currently is MSTW
- Current paradigm is to apply NLO uncertainty band to NNLO predictions from MSTW
 - basically a factor of 2 increase over MSTW errors by themselves

For CTEQ: α_s series

- Take CTEQ6.6 as base, and vary $\alpha_s(m_Z)$ +/-0.002 (in 0.001 steps) around central value of 0.118
- Blue is the PDF uncertainty from eigenvectors; green is the uncertainty in the gluon from varying α_s
- We have found that change in gluon due to α_s error (+/-0.002 range) is typically smaller than PDF uncertainty with a small correlation with PDF uncertainty over this range
  - as shown for gluon distribution on right
- **PDF error and α_s error can be added in quadrature**
  - expected because of small correlation
  - in recent CTEQ paper, it has been proven this is correct regardless of correlation, within quadratic approximation to χ^2 distribution

arXiv:1004.4624; PDFs available from LHAPDF

So the CTEQ prescription for calculating the total uncertainty (PDF+α_s) involves the use of the 45 CTEQ6.6 PDFs and the two extreme α_s error PDF's (0.116 and 0.120)

Parton = g, Q=85.
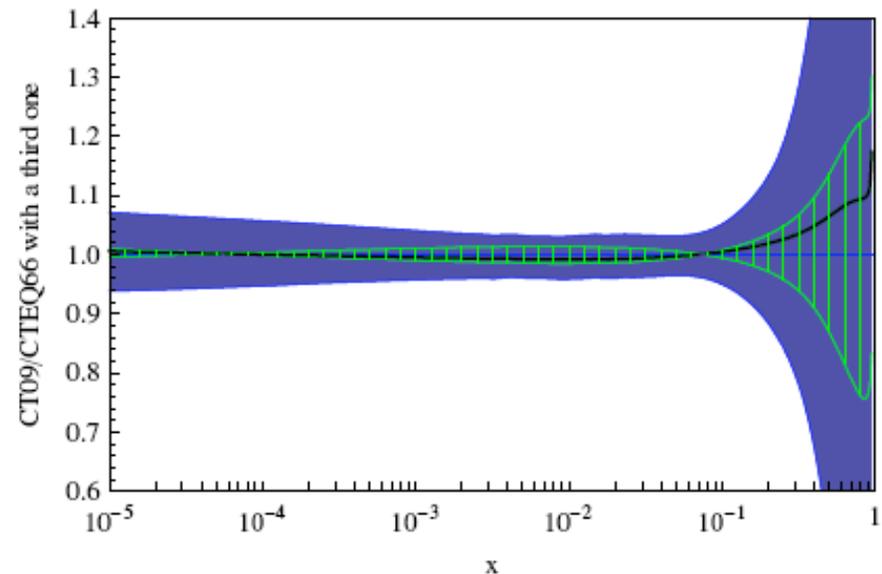
This also means that one can naively scale between 68% and 90% CL.

# New from CTEQ-TEA (Tung et al)->CT10 PDFs

- Combined HERA-1 data
- CDF and D0 Run-2 inclusive jet data
- Tevatron Run 2 Z rapidity from CDF and D0
- W electron asymmetry from CDFII and D0II (D0 muon asymmetry) (in CT10W)
- Other data sets same as CTEQ6.6
- All data weights set to unity (except for CT10W)
- Tension observed between D0 II electron asymmetry data and NMC/BCDMS data
- Tension between D0 II electron and muon asymmetry data

- Experimental normalizations are treated on same footing as other correlated systematic errors
- More flexible parametrizations: 26 free parameters (26 eigenvector directions)
- Dynamic tolerance: look for 90% CL along each eigenvector direction
  - within the limits of the quadratic approximation, can scale between 68% and 90% CL with naïve scaling factor
- Two series of PDF's are introduced
  - CT10: no Run 2 W asymmetry
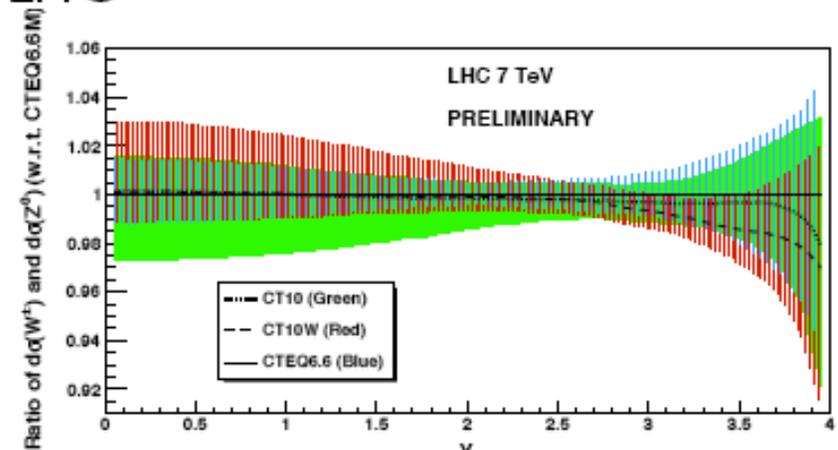 - CT10W: Run 2 W asymmetry with an extra weight

CT10/CT10W predictions

No big changes with respect to CTEQ6.6

Total cross sections

$\sigma(W^+)/\sigma(W^-)$ vs. y_W at the LHC
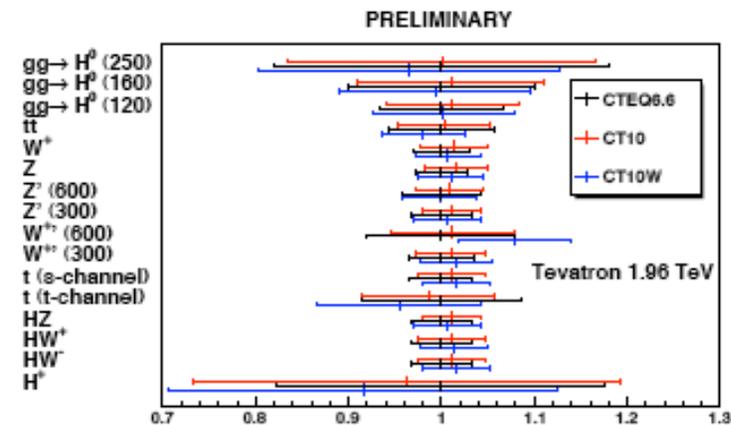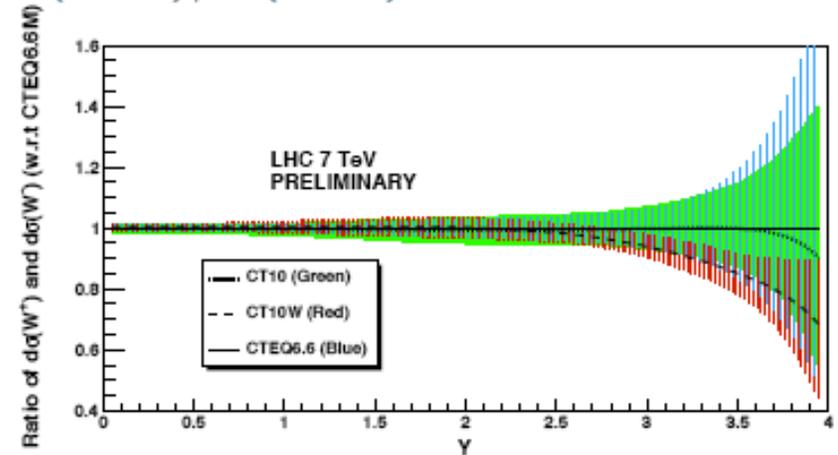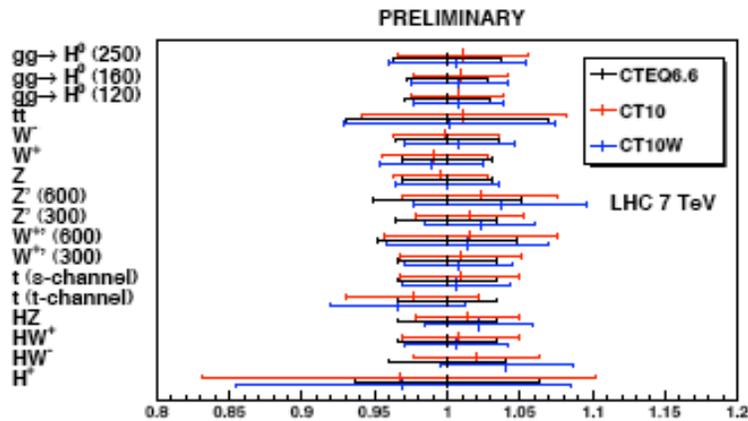
$\sigma(W^\pm)/\sigma(Z^0)$ vs. $y_{W/Z}$ at the LHC

LO PDFs

- Workhorse for many predictions at the LHC are still LO PDFs

- Many LO predictions at the LHC differ significantly from NLO predictions, not because of the matrix elements but because of the PDFs

- W^+ rapidity distribution is the poster child
  - the forward-backward peaking obtained at LO is an artifact
  - large x u quark distribution is higher at LO than NLO due to deficiencies in the LO matrix elements for DIS
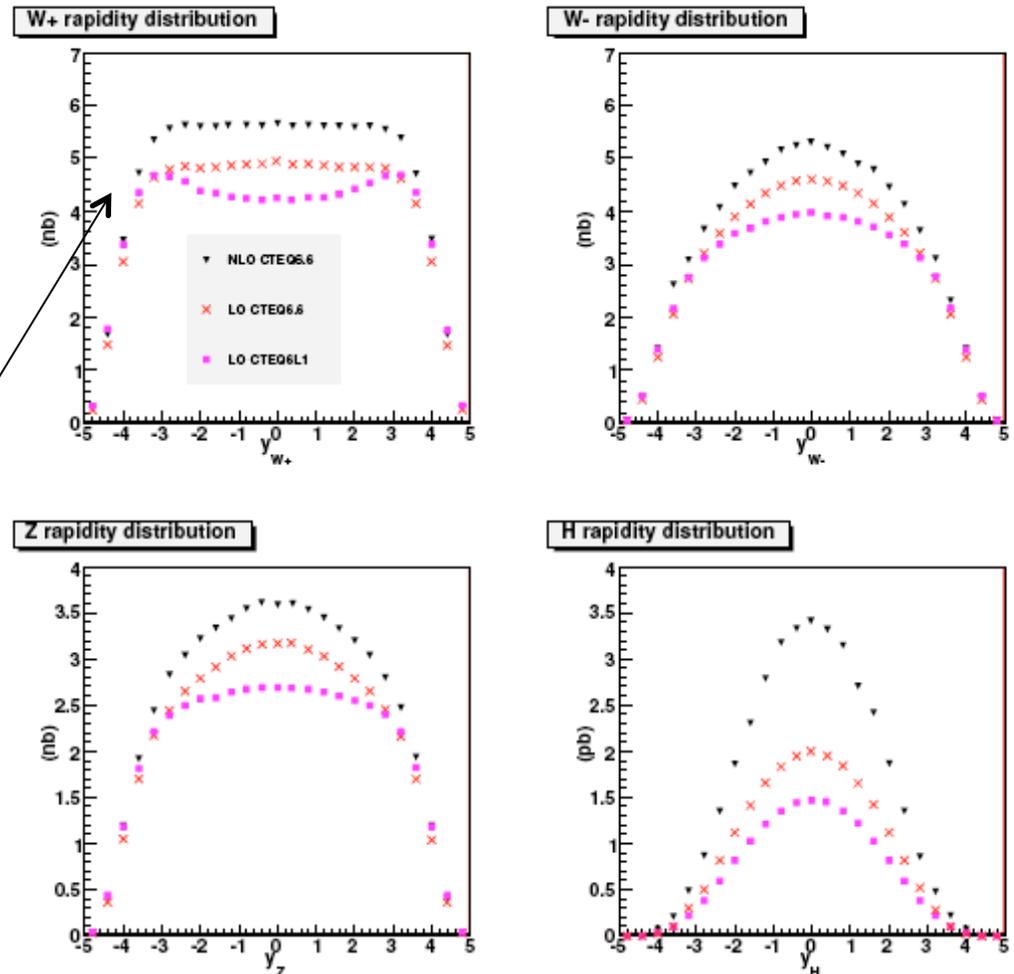

Figure 1. A comparison of the NLO pseudodata for SM boson rapidity distributions (in Δy=0.4 bins) predicted at the LHC (14 TeV) to the respective LO predictions based on CTEQ6.6M and CTEQ6L1 PDFs.

Modified LO PDFs

- Try to make up for the deficiencies of LO PDFs by
  - relaxing the momentum sum rule
  - including NLO pseudo-data in the LO fit to guide the modified LO distributions
- Results tend to be in better agreement with NLO predictions, both in magnitude and in shape
- Some might say that the PDFs then have no predictive power, but this is true for any LO PDFs

- See arXiv:0910.4183; PDFs available from LHAPDF
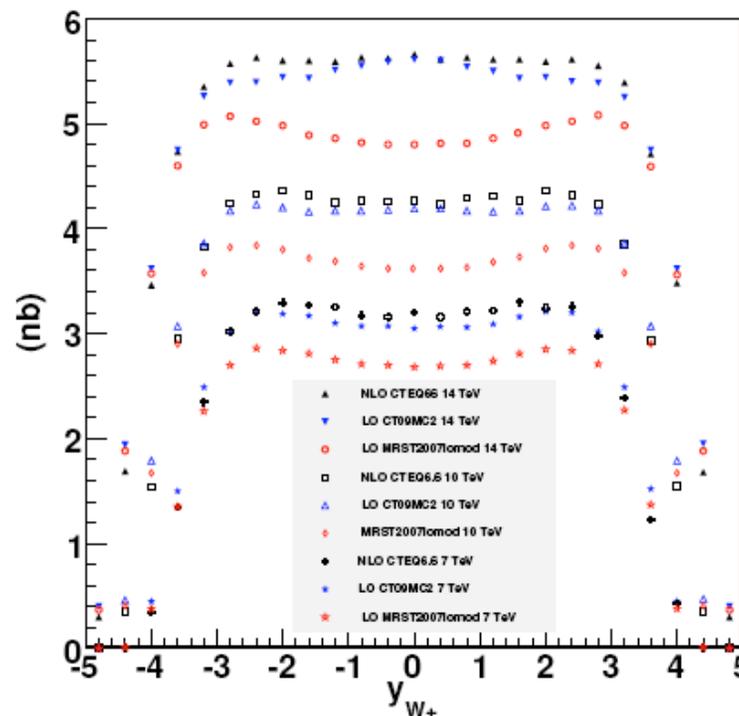- See arXiv:0711.2473 for MRST2007lomod PDFs

Figure 6. Predictions for the W^+ rapidity distribution at the LHC ($\sqrt{s}$ =7, 10 and 14 TeV) in Δy =0.4 bins, given at NLO using the CTEQ6.6M PDFs, and at LO using the CT09MC2 and MRST2007lomod PDFs. The actual cross sections (without normalization rescaling factors) are shown.

gg->Higgs

- **Higgs K-factor is too large to absorb into PDFs (nor would you want to)**

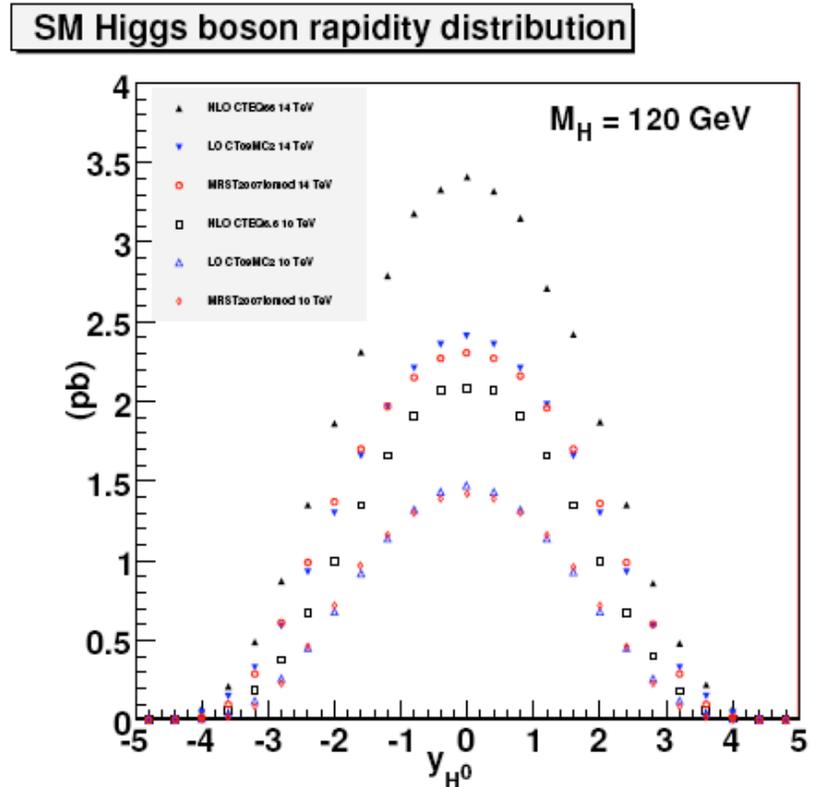- **Shape is ok with LO PDF's, improves a bit with the modified LO PDFs**

Figure 9. Same as figure 6, for the Higgs boson rapidity distribution at $\sqrt{s} =10$ and $14\,\text{TeV}$. To maintain legibility, the distribution for $\sqrt{s} =7\,\text{TeV}$ is not shown.